I R A M P
2(2), Dec. 2011, pp. 109-150

ISSN: 2229-3159

Evaluation of Van der Waals Broadening Data

A.V. DEMURA[a,b], S.YA. UMANSKII[b,c], A. V. SCHERBININ[b,d], A.V. ZAITSEVSKII[a,b]
G. V. DEMCHENKO[a.b], V. A. ASTAPENKO[b.e] AND B. V. POTAPKIN[a,b]

[a]Hydrogen Energy & Plasma Technology Institute, National Research Center "Kurchatov institute"
Kurchatov Square 1, Moscow 123182, Russia
[b]Kintech Laboratory Ltd., Kurchatov Square 1, Moscow 123182, Russia
[c]N.N. Semenov Institute of Chemical Physics RAS, Kosigina Street 4, Moscow 117992, Russia
[d]Faculty of Chemistry, Moscow State University, Leninskie Gory, Moscow 119991, Russia
[e]Department of Radio Engineering & Cybernetics, Moscow Physical and Technology Institute - State University
Dolgoprudniy, Institute alley 9, Moscow region 141700, Russia

ABSTRACT: Van der Waals broadening coefficients for numerous spectral transitions and radiator-perturber pairs are estimated by semi-empirical methods. The results are verified by *ab initio* electronic structure calculations and available experimental data. At the same time this allows to establish the range of applicability of Van der Waals approximation for interatomic potentials and description of broadening by atoms. The rigorous derivation of Van der Waals broadening characteristics in the impact regime is performed with the allowance for the degeneracy within the molecular basis in quasi-classical approximation, and the construction of the final Unified Frank-Condon profiles is outlined for binary broadening regimes.

Keywords: Van der Waals broadening with account of degeneracy, molecular basis, semi-empirical methods, *ab initio* electronic structure modeling

PACS: 31.15.bt, 31.15.bu, 31.15.A, 32.70.-n, 32.70.Jz, 34.20.-b, 34.20.Cf

1. INTRODUCTION

The data on Van der Waals broadening coefficients are requested in many applications, for example, in diagnostics of inductively coupled plasmas (ICP) [1], high intensity discharge lamps (HID) etc. [1-4]. However, those data are scarce in the up to date literature [2]. Indeed, there is a great number of papers, devoted to derivations of atom-atom potentials and in particular their approximate calculations within the perturbation theory [5], but very few works treat the case when one of the atoms is in the excited state [5]. Within this approximate perturbation representation of atom-atom interaction potential the first non-zero term is proportional to the inverse value of internuclear distance in the sixth power and used to be called Van der Waals or dispersion London-Lorentz interaction [5-6]. It is known from the first simplistic considerations of this case using atomic wave functions to build a zero order approximation, that this interaction depends on the sum of the atoms angular momentum projections on the internuclear axis [6]. Moreover, it was established, that the corresponding levels splitting is of the same order of magnitude as the interaction itself [6]. A more accurate zero-order approximation could be build of molecular wave functions [5], offering the possibility to improve the description of atom-atom interaction at any internuclear distances [5]. However, the latter would additionally require to go beyond perturbation theory approach in order to consider short-range contributions to the interaction potential [5]. Although the exact Van der Waals atom-atom interaction potential is generally anisotropic, for many years the theory of Van der Waals broadening was developing in the assumption of a scalar type of interaction, and this approximation was considered proven to be quite adequate for treating experimental results [7].

Here we present new extensive data on the Van der Waals broadening coefficients for numerous spectral transitions and many pairs of radiator and perturber atoms in the case of dispersion interaction between radiator and perturbing

particles at large distances, obtained by several methods of calculations. The comparison of the results, obtained by various methods is presented and the applicability of the Van der Waals approximation for the description of the atom-atom interaction potential for the excited states and calculations of broadening of atomic spectral lines are considered too. Besides the estimation of interaction potential itself this problem should include the assumptions on broadening regimes – impact [7], quasistatic or intermediate [6-9] depending on the relative velocities of interacting species. The study is performed within the adiabatic approximation providing quite sufficient accuracy for description of broadening by heavy particles for the most encountered conditions [7-10]. The performed tabulation encircles many identified spectral lines of various radiators although often exploits the data stored on Kurucz's CD 23 (see, for example, [11]), as the widely used NIST spectral database sometimes does not contain corresponding identification of specified transitions [12]. For testing the range of applicability and reliability of tabulated data obtained within semi-empirical approaches a few models, based on the *ab initio* electronic structure treatment, are developed to evaluate interaction potentials for identified radiative transitions for several diatomics, which include in some cases elements, possessing very high density of states like Nd and other lanthanide atoms. Those tests allow to elaborate modern methodology for description of spectral line broadening due to atom-atom interaction within Van der Waals approximation, based on the implementation of the molecular basis with recent advances in the theory of molecular spectral line broadening [13-15], model potentials [16-17] and various combinations of the wings cutting procedures, based on the notion of Massey parameter, widely used in the theory of atomic collisions (see, for example, [5]).

2. HYDROGEN-LIKE APPROXIMATION

For the sake of simplicity, let us consider the static interaction, temporally avoiding the discussion of interaction variations, arising from relative motion of radiator and perturber atoms [7-10]. For the situation involved in broadening many authors neglect the difference of excitation energies, corresponding to the radiator atom in the denominator of the general expression for the Van der Waals interaction coefficient C_6, in comparison with the energy differences of perturber atom [5-6]. If one additionally assumes that the angular momentum of the perturber atom in its ground state is equal to zero, the latter approximation allows to represent the C_6 in atomic basis as $C_6 \sim \alpha <r^2>$, where α is the polarizability of the perturber atom [5-6]. In the case when perturber is the same sort of atom as radiator this expression should be divided by 2 [5-6]. In this expression $<r^2>$ is taken over the radiator atom excited state "*i*". The further approximations concern the evaluation of contribution to $< r^2 > = < i | \left(\sum_{j=1}^{N} r_j \right)^2 | i >$ (*N* is the number of atomic electrons) from different atomic shells, where the contribution from closed atomic shells is considered conventionally negligible in comparison with that of the excited states from open shells [5-6]. Then $<r^2>$ could be approximately estimated from the expression for hydrogen-like system with the effective principal quantum number n_{eff}, defined by the experimental energy values of excited E_I states as $(n_{eff})^2 = Ry / |E_I|$, where E_I is counted off the continuum position. Then the mean square radius (MSR) of atomic state *nl* is given by the following expression

$$\left\langle nl \left| r^2 \right| nl \right\rangle_{HLA} = \frac{n_{eff}^2}{2} \left[5 n_{eff}^2 + 1 - 3l(l+1) \right]. \qquad (1)$$

This set of approximations for $\boldsymbol{C_6}$ calculations was called "hydrogen-like approximation" (HLA) [1-6] and seems to be firstly proposed by Albrecht Unzöld [18]. It gives quite reasonable results even in cases, when its rigorous formal application is not justified [18]. This formula was used to estimate Van der Waals broadening coefficients in many publications on applied spectroscopy [1-4]. In the present work we performed **HLA** calculations firstly for the external atomic shell, and then adding successively contributions from more inner shells, whilst the sequence of magnitudes of corresponding contributions allows to deduce the accuracy and convergence of results for $\boldsymbol{<r^2>}$, depending on particular atomic shells accounted for. The principal point and at the same time the main difficulty here is the definition of the ionization electron energy E_I, because in general this value is not equal to the ionization potential *I* of the atom. It should be taken either from the self-consistent Hartree-Fock atomic calculations or from experimental measurements. Usually the latter semi-empirical way is used more often and shown more

reliable. Evidently inner shells have larger binding energies and thus much smaller effective principal quantum numbers, that lead within HLA to much smaller and therefore negligible in comparison with outer shells contributions to $\langle r^2 \rangle$. Moreover, the outer shells with principal quantum numbers, equal to the corresponding one of excited level, provide the larger contributions to value of $\langle r^2 \rangle$.

To demonstrate relations between contribution from various shells let us consider for instance **Zn** ($Z = 30$) atom, which ground state configuration is **$4s^2$ ($^1S_0$)**. Its first excited configurations are …**3d104s4p** and ….**3d104s4d**. For the first configuration the contribution of 4s is 4.17 and 4p is 9.74, and for the second one – **4s** gives 2.99 and **4d** - 106.56 in squared atomic units of length. Qualitatively it is quite reasonable as the electron with a larger angular momentum shields weaker the inner electron with a lesser momentum, and therefore the latter has a larger binding energy and a smaller contribution to $\langle r^2 \rangle$.

Another test of the hydrogen-like approximation could be performed using the experimental measurements and calculations presented in [19] for **Tl** ($Z = 81$), whose ground state configuration is **$6s^26p$ ($^2P_{1/2}$)**. The line 377.68 nm $7s^2\ S_{1/2} - 6p\ ^2P_{1/2}$ of **Tl** atom was under investigation. The value of $\left\langle r^2 \right\rangle$ was taken from [20]. The calculations for the ground state $6p^2\ P_{1/2}$ are summarized just hereinafter:

Method	$\left\langle r^2 \right\rangle$, *a.u.*	C_6, 10^{-31} cm^6 rad s^{-1}
Hydrogen-like conventional method (for one electron)	6.84	1.68
Hydrogen-like semi-empirical method (this work)	14.13	3.47
Reference book [20]	17.7	4.35
Coulomb [19]	-	1.68
HF [21]	-	4.38
DHF [22]	-	3.52

It is worthy to note that the value from [20] is close to the **HF** value, obtained in [19] with non-relativistic Hartree-Fock wave functions using program [21]. The conventional **HLA** procedure is equivalent to the "Coulomb" column. The method proposed in this work provides a good agreement with values obtained in frames of more sophisticated approaches like called in [19] **HF** and **DHF** values, the latter one being obtained in [19] with multiconfiguration relativistic Dirac-Hartree-Fock wave functions using program, elaborated in [22].

For the excited state $7s\ ^2S_{1/2}$ the data are presented below:

Method	$\left\langle r^2 \right\rangle$, *a.u.*	C_6, 10^{-31} cm^6 rad s^{-1}
Hydrogen-like conventional method (for one electron)	60.38	14.8
Hydrogen-like semi-empirical method (this work)	64.91	15.9
DHF [22]	-	18.0

As it is seen from the above comparison **HLA** provides quite reasonable results for C_6 even for the ground state of **Tl**. As to the comparison of the impact broadening width in the adiabatic approach [7] with experiment, given below, as explained above it is convincing even more, than the comparison of C_6.

Comparison with the experimental values of impact broadening

Method	*Impact width* γ, 10^{-20} cm^3 cm^{-1}
Hydrogen-like semi-empirical method (this work)	3.04
DHF [22]	3.19
Experiment [19]	3.19

Thus it could be concluded that the HLA semi-empirical method with account of 3 electrons provides a rather good agreement for all considered states of Tl, once more confirming the applicability of HLA in general.

2.1. HLA Refinement with Green-Selin-Zachor Model Potential

One of the obvious ways to improve HLA consists in calculating $\langle r^2 \rangle$ without resorting to the hydrogen – like expression. A good candidate for that is the Green-Selin-Zachor model atomic core potential (GSZ) in the electron location, tabulated practically for all elements of periodic table [16]

$$U_{GSZ}(r) = -\frac{2 \cdot \zeta(r)}{r},\ \zeta(r) = 1 + \frac{Z-1}{1 + p \cdot (Z-1)^{0.4} \left[\exp(r/p) - 1\right]} \tag{2}$$

Here $\zeta(r)$ is the effective charge, p is the potential numerical parameter, tabulated for all elements, Z is the charge number of atomic nucleus, the dimensionless radial distance r is expressed in terms of atomic units.

Using (2) and the experimental energy values, the Schroedinger equation is solved numerically with the appropriate GSZ potential, and the corresponding wave functions $P_{nl}(r)$ are obtained for known identified energy levels

$$\left[\frac{d^2}{dr^2} - \frac{l(l+1)}{r^2} + \frac{1}{\Lambda} U_{GSZ}\left(\frac{r}{\Lambda}\right) + \varepsilon\right] P_{nl}(r) = 0 \tag{3}$$

Here $\varepsilon = E_i$, n, l are assumed to be known. The radial wave function $P_{nl}(r)$ satisfies the asymptotic

$$P_{nl}(r \to 0) \propto r^{l+1};\ P_{nl}(r \to \infty) \propto r^{|\varepsilon|^{-0.5}} \exp\left(-\sqrt{|\varepsilon|}\, r\right) \tag{4}$$

and normalization conditions

$$\int_0^\infty P_{nl}(r) P_{n'l}(r)\, dr = \delta_{nn'} \tag{5}$$

Here $\varepsilon < 0$ is the experimental energy value in atomic units for bound state

$$|\varepsilon| = \frac{1}{2 n_{eff}^2}, \tag{6}$$

Λ is the scaling factor which should be chosen to satisfy the asymptotic behavior (4), $U_{GSZ}(r)$ is the potential energy of atomic core in Green-Selin-Zachor approximation, $\boldsymbol{l}$ is the orbital quantum number, $\delta_{nn'}$ is the Kronneker symbol. Numerical procedure utilizes the fourth order Runge-Kutta fixed step method for solving ordinary differential equations. Thus in frames of the proposed refinement the MSR $\langle r^2 \rangle = \langle nl | r^2 | nl \rangle$ of atomic state nl is calculated according to the formula

$$\langle nl | r^2 | nl \rangle = \int_0^\infty P_{nl}(r)^2\, r^2 dr \tag{7}$$

The comparison of GSZ results for $\langle r^2 \rangle$ with HLA ones for particular atomic shells shows a quite small difference, that will be illustrated below in this section. This approach obviously could be applied for calculations of contribution to MSR from any atomic shell. There are also examples of using less universal approaches, by introducing the dependence of GSZ-like pseudopotentials on the angular momentum of atomic shells in attempt to tune shielding factors [23]. For demonstrating the possibilities of GSZ approximation we performed calculations of broadening characteristics for several transitions of Na and Nd atoms, perturbed by Xe in the ground state. The calculations are

done only for the valence shells of Na and Nd radiators. The results of HLA spproximation for the outer electrons of Na and Nd are also presented for comparison. It is seen that the arising difference between two approximations is rather small.

Sodium atom, Z = 11, d = 0.561, I_{3s} = 5.14 eV, Xe atom as perturber

state	*3s*	*3p*	*4p*	*5p*	*6p*	*7p*
Energy above ground state, eV	0	2.1	3.753	4.344	4.624	4.779
Scaling factor	0.92644 x_{max}=30	0.90939 x_{max}= 40	0.904757 x_{max} = 60	0.90723 x_{max} = 80	0.909 x_{max} = 100	0.9055 x_{max} = 120
MRS, a.u.	19.322	39.739	217.253	688.954	1672	3455
MRS, a.u. (HLA)	18.825	38.85	215.848	687.066	1671	3454
$C_6 - C_6^{ground}$ for Xe, a.u.	-	551.257	5344	18120	44730	92960

Neodymium atom, Z = 60, d = 0.938, I_p = 5.525 eV, Xe atom as perturber

State	*$4f^4 6s^2$ ($^5I_6$)*	*$4f^4 6s^2$ ($^5I_5$)*	*$4f^4 6s6p$ $^5H_3^o$*	*$4f^4 6s6p$ $^5K_9^o$*	*$4f^4 6s6p$ $^5K_6^o$*	*$4f^4 6s6p$ $^5K_5^o$*	*Unknown X_1,*
Energy above ground state, eV	0	0.14	2.675	3.164	2.671	2.517	2.647
Orbital momentum quantum number	0	0	1	1	1	1	1
Scaling factor	1.1151 x_{max}=30	1.10858 x_{max}=30	0.98563 x_{max}=30	0.90106 x_{max}=30	0.98616 x_{max}=30	1.00523 x_{max}=30	0.98933 x_{max}=30
MRS, a.u.	21.31	21.933	48.458	72.173	48.341	43.498	47.323
MRS, a.u. (HLA)		17.209	44.998	68.551	44.856	39.802	44.012
$C_6 - C_6^{ground}$ for Xe, a.u.		734.621		1376	731.436	600.4	703.898

3. MOLECULAR BASIS

In this chapter the possibility to represent $\mathbf{C_6}$ using the molecular basis (MB) [5], that evidently is the most consistent basis for representing interaction of two neutral atoms, in a quite compact analytic form, where the sought coefficients are expressed through integrals of the product of reduced matrix elements of dynamic polarizabilities, extracting practically all general dependencies on values of angular momentum and their projections on internuclear axis, is demonstrated. Those matrix elements contain the sums over the various atomic states from different shells [5-6]. As usual, it is convenient to consider Hund cases "a" and "c" separately [5]. Conventionally and for simplicity, like in the case of HLA, the contributions from various shells are considered as additive [5-6]. However, the main contribution obviously comes from open outer atomic shells, that can not be found analytically in general case, especially for the shells with equivalent electrons [5]. In this work these entities for several types of outer atomic shells and particular perturbers were analyzed and evaluated with the help of the closure approximation [5]. In this approximation the difference of energies in the denominator and numerator in the expression for polarizability is substituted by the constant effective value of the energy difference, that should match the limit corresponding to Slater-Kirkwood approximation (see [24]). All this allows to structuralize in a general way the formulas for $\boldsymbol{C_6}$ coefficients and express each of additive terms similar to HLA as a product of the square of the effective radius of the excited electron orbital and the polarizability of the perturber in the ground state. To evaluate $\langle r^2 \rangle$ the GSZ model [16] also could be used.

3.1. Dispersion Interaction of Atoms in Degenerate Orbital States

Now we shall consider in detail dispersion interaction of the atom in an excited state (atom A - radiator) and perturbing (atom X - buffer) atom in the ground state, identifying orbital quantum numbers, that are necessary for constructing molecular basis [5]. In this basis the quantum transitions occur between the states of compound system of two atoms –diatom [5]. This transition evidently corresponds to particular quantum transitions of atom A

$$\mathbf{A}(\gamma_i j_i) \rightarrow \mathbf{A}(\gamma_f j_f) + h\mathbf{n}_0, \tag{8}$$

Here $\boldsymbol{j}_i$ and $\boldsymbol{j}_f$ are the quantum numbers of the total (orbital angular momentum + spin) angular momentum of the radiating atom A in the initial and final states, $\boldsymbol{\gamma}_i$ and $\boldsymbol{\gamma}_f$ are the sets of all other quantum numbers characterizing initial and final energy levels, and $\boldsymbol{\nu}_0$ is the cyclic frequency of the emitted photon. Always at least one of $\boldsymbol{j}_i$ and $\boldsymbol{j}_f$ is larger than zero for A with even number of electrons or than ½ for A with odd number of electrons. The removal of degeneracy of the radiating state of atom A with $\boldsymbol{j}>\mathbf{0}$ or ½ due to the interaction with the approaching atom X, leads to the onset of several potential curves of the A–X compound system. In particular, several dispersion interactions $\sim\mathbf{1}/\boldsymbol{R}^6$ ($\boldsymbol{R}$ is A–X internuclear distance) exist at large $\boldsymbol{R}$ in this case.

The problem of the interatomic dispersion interaction evaluation is rather minutely discussed in literature (see, e. g. [5], and references therein), where the explicit expressions for dispersion interaction are derived in terms of quantum characteristics of radiating and buffer atoms, Hund case "**a**". Here we shall modify those results, that are necessary for our further analysis of the state degeneracy and for performing calculations of Van der Waals broadening for Hund case "**c**". It should be underlined that although the representation of these results here has several conventional main features it is original enough in totality.

The dispersion (Van der Waals) interaction is due to dipole-dipole interaction

$$V_{\mathrm{AX},dd} = -\frac{2}{R^3}\sum_{q=-1}^{1}\frac{1}{(1-q)!(1+q)!}D_{q\mathrm{A}}D_{-q\mathrm{X}} \tag{9}$$

in the second-order of perturbation theory [5-6]. Here $\boldsymbol{R}$ is internuclear distance, and $\boldsymbol{D}_{q\mathrm{A}}$, $\boldsymbol{D}_{-q\mathrm{X}}$ are the spherical components of dipole moment operators for atoms A and X respectively.

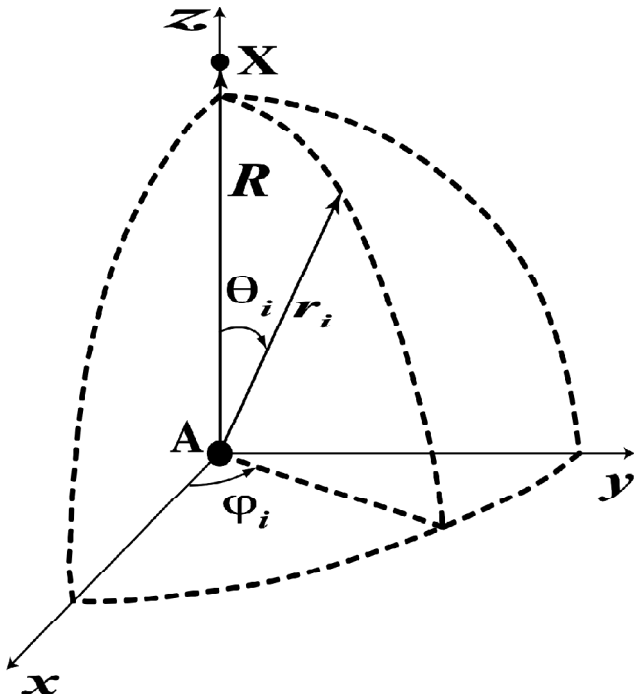

Figure 1: Reference frame in which the dipole-dipole interaction (9) is defined

The spherical components of operator $\boldsymbol{D}_{qA}$ (or analogously $\boldsymbol{D}_{-qX}$) are defined as follows

$$D_{qA} = -e\sum_{i}^{N_A} r_i \left(\frac{4\pi}{3}\right)^{1/2} Y_1^q(\theta_i, \varphi_i) = \sum_{i}^{N_A} D_{qA}(\theta_i, \varphi_i). \tag{10}$$

Here e is the electron charge, $\boldsymbol{N}_A$ is the number of electrons in the atom A, $\boldsymbol{r}_i$, $\boldsymbol{\theta}_i$, $\boldsymbol{\varphi}_i$ are the spherical coordinates of the ith electron of the atom A in coordinate frame, whose z axis is directed along vector $\boldsymbol{R}$ from the A nucleus to the X one, and whose origin is at the A nucleus (see Fig. 1), and $Y_1^q(\theta_i, \varphi_i)$ is the spherical function.

Using the well known relation [5]

$$\frac{1}{a+b} = \frac{2}{\pi}\int_0^\infty \frac{ab}{(a^2+\omega^2)(b^2+\omega^2)} d\omega \tag{11}$$

the matrix element of dispersion interaction between the molecular state $<\gamma_A\gamma_X J\tilde{\Omega}|$ and the state $|\gamma_A'\gamma_X' J'\tilde{\Omega}'>$ with the projections $\hbar\tilde{\Omega}, \hbar\tilde{\Omega}'$ of total angular momentum on the $\boldsymbol{z}$ axis defined in the Fig. 1 could be given by the following expression

$$\begin{aligned} &<\gamma_A\gamma_X J\tilde{\Omega}|V^{(2)}_{AX,dd}(R)|\gamma_A'\gamma_X' J'\tilde{\Omega}'> = -\delta_{\tilde{\Omega}\tilde{\Omega}'} R^{-6} \times \\ &\sum_{m_{JA}, m_{JX}} \sum_{m'_{JA}, m'_{JX}} \begin{bmatrix} J_A & J_X & J \\ m_{J_A} & m_{J_X} & \tilde{\Omega} \end{bmatrix} \times \begin{bmatrix} J'_A & J'_X & J' \\ m'_{J'_A} & m'_{J'_X} & \tilde{\Omega}' \end{bmatrix} \times \sum_{qq'} [(1-q)!(1+q)!(1-q')!(1+q')!]^{-1} \\ &\times \frac{2}{\pi}\int_0^\infty \left\langle \gamma_A J_A m_{J_A} \left| \alpha^{(11)}_{qq'A}(\omega) \right| \gamma_A' J_A' m'_{J'_A} \right\rangle \left\langle \gamma_X J_X m_{J_X} \left| \alpha^{(11)}_{-q-q'X}(\omega) \right| \gamma_X' J_X' m'_{J'_X} \right\rangle d\omega \end{aligned} \tag{12}$$

where symbol like $\begin{bmatrix} J_A & J_X & J \\ m_{J_A} & m_{J_X} & \tilde{\Omega} \end{bmatrix}$ designates Glebsh-Gordon coefficient. In the case of diagonal matrix elements for atom A the first multiplier in the integrand over ω in (12) has the form

$$\begin{aligned} &\left\langle \gamma_A J_A m_{J_A} \left| \alpha^{(11)}_{qq'A}(\omega) \right| \gamma_A J_A m_{J_A} \right\rangle = 2 \sum_{\gamma_A^* J_A^* \neq \gamma_A J_A} \sum_{m_{J_A}^*} \frac{\varepsilon_{\gamma_A^* J_A^*} - \varepsilon_{\gamma_A J_A}}{(\varepsilon_{\gamma_A^* J_A^*} - \varepsilon_{\gamma_A J_A})^2 + \hbar^2\omega^2} \times \\ &\times \left\langle \gamma_A J_A m_{J_A} \left| D^{(1)}_{qA} \right| \gamma_A^* J_A^* m_{J_A}^* \right\rangle \left\langle \gamma_A^* J_A^* m_{J_A}^* \left| D^{(1)}_{qA} \right| \gamma_A J_A m_{J_A} \right\rangle , \end{aligned} \tag{13}$$

and similarly in the same case the second multiplier in the integrand in (12) for atom X is expressed as

$$\begin{aligned} &\left\langle \gamma_X J_X m_{J_X} \left| \alpha^{(11)}_{-q-q'X}(\omega) \right| \gamma_X J_X m_{J_X} \right\rangle = 2 \sum_{\gamma_X^* J_X^* \neq \gamma_X J_X} \sum_{m_{J_X}^*} \frac{\varepsilon_{\gamma_X^* J_X^*} - \varepsilon_{\gamma_X J_X}}{(\varepsilon_{\gamma_X^* J_X^*} - \varepsilon_{\gamma_X J_X})^2 + \hbar^2\omega^2} \times \\ &\times \left\langle \gamma_X J_X m_{J_X} \left| D^{(1)}_{-qX} \right| \gamma_X^* J_X^* m_{J_X}^* \right\rangle \left\langle \gamma_X^* J_X^* m_{J_X}^* \left| D^{(1)}_{-q'X} \right| \gamma_X J_X m_{J_X} \right\rangle. \end{aligned} \tag{14}$$

In (13)-(14) $\varepsilon_{\gamma_A^* J_A^*}, \varepsilon_{\gamma_A J_A}, \varepsilon_{\gamma_X^* J_X^*}, \varepsilon_{\gamma_X J_X}$ are the corresponding energy levels of atoms A and X, and the quantities $\left\langle \gamma_A J_A m_{J_A} \left| \alpha^{(11)}_{qq'A}(\omega) \right| \gamma_A J_A m_{J_A} \right\rangle$ and $\left\langle \gamma_X J_X m_{J_X} \left| \alpha^{(11)}_{-q-q'X}(\omega) \right| \gamma_X J_X m_{J_X} \right\rangle$ are atomic dipole polarizabilities at imaginary frequency $i\omega$.

The operator $\alpha^{(11)}_{qq'\mathrm{A}}(\omega)$, defined by (14), transforms under rotations as the direct product of two irreducible tensor operators of rank 1. It is convenient to introduce irreducible tensor operators

$$\alpha^{(\chi)}_{m\mathrm{A}}(\omega) = \sum_{qq'} \begin{bmatrix} 1\ 1\ \chi \\ q\ q'\ m \end{bmatrix} \alpha^{(11)}_{qq'\mathrm{A}}(\omega), \tag{15}$$

where $\begin{bmatrix} 1\ 1\ \chi \\ q\ q'\ m \end{bmatrix}$ are Klebsch-Gordan coefficients and χ can assume the values 0, 1, and 2, and evidently similarly for atom *X*. Correspondingly, the polarizability of the atom *A* or *X* in the degenerate state is defined by three reduced matrix elements $\langle \gamma j \| \alpha^{(\chi)}_{\mathrm{A,X}}(\omega) \| \gamma j \rangle$ with χ = 0, 1, 2. We prefer to use the definition of the reduced matrix elements from [7]. In the same way the irreducible tensor operators can be introduced for the atom *X*. Rearranging (13) and (14) using (15), the following expression for the reduced matrix elements is obtained

$$\begin{aligned} \langle \gamma j \| \alpha^{(\chi)}_{\mathrm{A}}(\omega) \| \gamma j \rangle = (2\chi+1)^{1/2}(-1)^{j+\chi} \sum_{\gamma^* j^* \neq \gamma j} \frac{\varepsilon_{\gamma^* j^*} - \varepsilon_{\gamma j}}{(\varepsilon_{\gamma^* j^*} - \varepsilon_{\gamma j})^2 + \hbar^2\omega^2} \times \\ \times (-1)^{j^*} \begin{Bmatrix} j^* 1\ j \\ \chi\ \ j'\ 1 \end{Bmatrix} |\langle \gamma j \| D^{(1)}_{\mathrm{A}} \| \gamma^* j^* \rangle|^2 , \end{aligned} \tag{16}$$

where we suppressed subscript "*A*" for "γ" and "*J*", and substituted capital "*J*" by small one "*j*" for simplicity. The notation $\begin{Bmatrix} j^* 1\ j \\ \chi\ \ j'\ 1 \end{Bmatrix}$ is Wigner 6-j symbol, and $\langle \gamma j \| D^{(1)}_{\mathrm{A}} \| \gamma^* j^* \rangle$ is the reduced matrix elements of the dipole moment. In particular

$$\langle \gamma j \| \alpha^{(0)}_{\mathrm{A}}(\omega) \| \gamma j \rangle = -3 \left(\frac{2j+1}{3} \right)^{1/2} \alpha_{\gamma j\mathrm{A}}(\omega), \tag{17}$$

where

$$\alpha_{\gamma j\mathrm{A}}(\omega) = \sum_{m_{J_A}} (2j+1)^{-1} \langle \gamma j m_{J_A} | \alpha^{(11)}_{00\mathrm{A}}(\omega) | \gamma j m_{J_A} \rangle \tag{18}$$

is the polarizability of atom A in an electric field, directed along the *z* axis, and averaged over all degenerate states. Analogously the irreducible tensor operators can be introduced for the atom X.

Using the representation of reduced matrix elements of polarizability (15), the general expression for Van der Waals interaction in the Hund case "c" takes the form (compare with (4.52) for Hund case "a"in [5])

$$\begin{aligned} < \gamma_A \gamma_X J\tilde{\Omega} | V^{(2)}_{AX,dd}(R) | \gamma'_A \gamma'_X J'\tilde{\Omega}' > = -\delta_{\Omega\Omega'} R^{-6} \times \\ \sum_{\chi} \sum_{\chi_A} \sum_{\chi_X} \sum_{qq'} [(1-q)!(1+q)!(1-q')!(1+q')!]^{-1} \\ \times \begin{bmatrix} 1 & 1 & \chi_A \\ q & q' & q+q' \end{bmatrix} \times \begin{bmatrix} 1 & 1 & \chi_X \\ -q & -q' & -q-q' \end{bmatrix} \times \begin{bmatrix} \chi_A & \chi_X & \chi \\ q+q' & -q-q' & 0 \end{bmatrix} \\ \times \begin{bmatrix} J' & \chi & J \\ \tilde{\Omega}' & 0 & \tilde{\Omega} \end{bmatrix} \begin{Bmatrix} \chi & J & J' \\ \chi_A & J_A & J'_A \\ \chi_X & J_X & J' \end{Bmatrix} \times \alpha_{AX}(\chi_A, \chi_X), \end{aligned} \tag{19}$$

where {...} is the 9-j symbol, and the quantity $\alpha_{AX}(\chi_A, \chi_X)$ is defined evidently as

$$\alpha_{AX}(\chi_A,\chi_X) = \frac{2}{\pi}\int_0^\infty \left\langle \gamma_A \left\| \alpha_{\mathrm{A}}^{(\chi_A)}(\omega) \right\| \gamma'_A \right\rangle \left\langle \gamma_X \left\| \alpha_{\mathrm{X}}^{(\chi_X)}(\omega) \right\| \gamma'_X \right\rangle d\omega, \tag{20}$$

where $\left\langle \gamma_A \left\| \alpha_{\mathrm{A}}^{(\chi_A)}(\omega) \right\| \gamma'_A \right\rangle$, $\left\langle \gamma_X \left\| \alpha_{\mathrm{X}}^{(\chi_X)}(\omega) \right\| \gamma'_X \right\rangle$ are the reduced matrix elements of the polarizability tensor.

It is known that additive terms in (19), containing α_{AX} for combinations of $(\chi_{\mathrm{A}}, \chi_{\mathrm{X}})$ - (1,0), (0,1),(1,2),(2,1), are equal to zero (see [5]), and thus (19) in the general Hund case "c" is determined by five independent parameters $\alpha_{\mathrm{AX}}(0,0)$, $\alpha_{\mathrm{AX}}(1,1)$, $\alpha_{\mathrm{AX}}(2,2)$, $\alpha_{\mathrm{AX}}(0,2)$ and $\alpha_{\mathrm{AX}}(2,0)$.

The Eq. (12)–(20) are all that could be obtained using only general formulas of the second order perturbation theory and the symmetry properties of atomic states.

3.2. Buffer Gas with Zero Total Angular Momentum of Ground State

In the case when the ground state of buffer gas atom *X* has zero angular momentum (^1S) the above expressions are greatly simplified. For instance the Eq (12) transforms to

$$V^{(d)}_{\gamma j\tilde{\Omega}}(R) = -R^{-6}\sum_{qq'}[(1-q)!(1+q)!(1-q')!(1+q')!]^{-1} \times \frac{2}{\pi}\int_0^\infty \left\langle \gamma j\tilde{\Omega}\left| \alpha^{(11)}_{qq'\mathrm{A}}(\omega)\right|\gamma j\tilde{\Omega}\right\rangle \left\langle {}^1S\left|\alpha^{(11)}_{-q-q'\mathrm{X}}(\omega)\right|{}^1S\right\rangle d\omega, \tag{21}$$

where

$$\left\langle \gamma j\tilde{\Omega}\left| \alpha^{(11)}_{qq'\mathrm{A}}(\omega)\right|\gamma j\tilde{\Omega}\right\rangle = 2\sum_{\gamma^* j^*\neq\gamma j}\sum_{\tilde{\Omega}^*}\frac{\varepsilon_{\gamma^* j^*}-\varepsilon_{\gamma j}}{(\varepsilon_{\gamma^* j^*}-\varepsilon_{\gamma j})^2+\hbar^2\omega^2}\times\left\langle \gamma j\tilde{\Omega}\left|D^{(1)}_{q\mathrm{A}}\right|\gamma^* j^*\tilde{\Omega}^*\right\rangle\left\langle \gamma^* j^*\tilde{\Omega}^*\left|D^{(1)}_{q\mathrm{A}}\right|\gamma j\tilde{\Omega}\right\rangle.$$

$$\left\langle {}^1S\left|\alpha^{(11)}_{-q-q'\mathrm{X}}(\omega)\right|{}^1S\right\rangle = 2\sum_{\beta^*}\frac{\varepsilon_{\beta^*}-\varepsilon_{{}^1S}}{(\varepsilon_{\beta^*}-\varepsilon_{{}^1S})^2+\hbar^2\omega^2}\left\langle {}^1S\left|D^{(1)}_{-q\mathrm{X}}\right|\beta^*\right\rangle\left\langle\beta^*\left|D^{(1)}_{-q'\mathrm{X}}\right|{}^1S\right\rangle. \tag{22}$$

Since the atom *X* is in the nondegenerate state with zero angular momentum, only the irreducible matrix element $\left\langle {}^1S\,\|\alpha^{(0)}_{\mathrm{X}}(\omega)\|\,{}^1S\right\rangle$ will appear in the final expression for the dispersion interaction

$$\left\langle {}^1S\,\|\alpha^{(0)}_{\mathrm{X}}(\omega)\|\,{}^1S\right\rangle = -\sqrt{3}\alpha_{{}^1SX}(\omega) \tag{23}$$

Using the reduced matrix elements $\left\langle \gamma j\,\|\alpha^{(\chi)}_{\mathrm{A}}(\omega)\|\,\gamma j\right\rangle$ and $\left\langle {}^1S\,\|\alpha^{(0)}_{\mathrm{X}}(\omega)\|\,{}^1S\right\rangle$, the expression (21) for dispersion interaction could be rewritten in the following somewhat universal form, suitable for further considerations,

$$V^{(d)}_{\gamma j\tilde{\Omega}}(R) = -\frac{C_6^{(0,j\gamma)}}{R^6}\left[1-B_6^{(2,j\gamma)}\begin{bmatrix} j & 2 & j\\ \tilde{\Omega} & 0 & \tilde{\Omega}\end{bmatrix}\right], \tag{24}$$

where

$$C_6^{(0,j\gamma)} = \frac{1}{\pi(2j+1)^{1/2}}\int_0^\infty\left\langle \gamma j\,\|\alpha^{(0)}_{\mathrm{A}}(\omega)\|\,\gamma j\right\rangle\left\langle {}^1S\,\|\alpha^{(0)}_{\mathrm{X}}(\omega)\|\,{}^1S\right\rangle d\omega, \tag{25}$$

and

$$B_6^{(2,j\gamma)} = \frac{\int_0^\infty \langle \gamma j \| \alpha_A^{(2)}(\omega) \| \gamma j \rangle \langle {}^1S \| \alpha_X^{(0)}(\omega) \| {}^1S \rangle d\omega}{\sqrt{2}\int_0^\infty \langle \gamma j \| \alpha_A^{(0)}(\omega) \| \gamma j \rangle \langle {}^1S \| \alpha_X^{(0)}(\omega) \| {}^1S \rangle d\omega}. \quad (26)$$

There is enormous number of works devoted to calculations of static and dynamic atomic polarizabilities (see [23, 25-39] and reference therein) and related to them constants of Van der Waals atom-atom interactions [23-24, 28, 33-39], that includes in particular the many-body perturbation theory [25-27], time-dependent Hartree-Fock [28-29], variational methods [30] and time dependent Local Density Functional Theory [30-31]. Besides these direct methods there are semi-empirical methods that use additionally known experimental data [20, 39]. However, at the same time the tabulated data are still kept scarce [20, 23-39]. Moreover, amazingly we did not even find contemporary reviews, that would comprehensively enough summarize the current situation in this field. On the other hand it is not our goal to review here the various methods of those calculations that are kept quite laborious up to now. It is important to underline that in distinction from recent works on the subject [35-38], which are aimed on increasing the accuracy of calculations including various very subtle relativistic effects and peculiarities in the summation over virtual states [37-38], which takes into account correlations between various shells and use experimental values of oscillator strengths [38], the data for description of atomic broadening under study here are obtained in assumption of additivity of contributions from different shells and do not require so high level of accuracy as, for instance, in [37-38]. However, the mentioned broadening data, we are interested in, could be obtained by more simplified semi-empirical procedures (see for instance [5, 20, 24]), but for their accuracy it is more important to consider the characteristics of particular quantum transitions for upper and lower levels on the equal footing.

Indeed, a rather reliable evaluation of $\alpha_{AX}(\chi_A, \chi_X)$ could be accomplished with the additional conventional approximations (see, for instance, [5]), itemized as follows.

1. The LS-coupling takes place for states $(\gamma_i j_i)$ and $(\gamma_f j_f)$ of the radiating atom A.
2. The energy differences in (13)-(14) and (16) are substituted by the constant average values of $\Delta\varepsilon_A \equiv \overline{\varepsilon_{\gamma_A^* J_A^*} - \varepsilon_{\gamma_A J_A}}$ and $\Delta\varepsilon_X \equiv \overline{\varepsilon_{\gamma_X^* J_X^*} - \varepsilon_{\gamma_X J_X}}$ (so called - closure approximation). The average excitation energies are of the order of the ionization energies of the corresponding atomic states. The specific values are to be selected basing on the additional physical arguments (see [5]).
3. Often it is assumed that polarizability of the atom A is determined by its outer electronic shell.

It is interesting that if to adopt the first two approximations, then one could start with the expressions for Van der Waals interaction for the Hund cases “a” [5] instead of presented here case “c”.

Now consider, for example, the important for applications case of metal atoms A with only one outer electron above closed inner electronic shells, determining its visible spectrum. In this case the set γ, determining energy levels of the optical electron, includes the orbital quantum number ℓ and the principle quantum number n, i.e. $\gamma = \{n, \ell\}$. With the above approximations the following expressions for $C_6^{(0,jn\ell)}$ and $B_6^{(2,jn\ell)}$ are obtained with the help of elementary theory of residues, used in derivation of relation (11) too,

$$C_6^{(0,jn\ell)} = \alpha_X \left\langle r_{n\ell,A}^2 \right\rangle \frac{\Delta\varepsilon_X}{\Delta\varepsilon_{n\ell,A} + \Delta\varepsilon_X}, \quad (27)$$

$$B_6^{(2,jn\ell)} = (-1)^{\ell+\frac{1}{2}+j+1} \sqrt{(2\ell+1)(2j+1)} \begin{bmatrix} \ell & 2 & \ell \\ 0 & 0 & 0 \end{bmatrix} \begin{Bmatrix} \ell & j & 1/2 \\ j & \ell & 2 \end{Bmatrix} \quad (28)$$

Here α_X is the static dipole polarizability of $X(^1S)$ and $\left\langle r^2_{n\ell,A} \right\rangle$ is a mean square radius of the outer orbital $\varphi_{n\ell}(r)$ of A. For instance, the quantity $\left\langle r^2_{n\ell,A} \right\rangle$ also could be reasonably estimated in the framework of effective atomic core **GSZ** model potential [3], referred above.

Often for the estimates of dispersion interaction - the described above **HLA** [4] is used, which in frames of MB approach assumes additionally to approximations 1-2 that,

(a) the quantity $B_6^{(2,jn\ell)}$ can be neglected in comparison with unity;

(b) $\Delta\varepsilon_{n\ell,A}$ could be neglected in comparison with $\Delta\varepsilon_X$ in (23);

(c) $\left\langle r^2_{n\ell,A} \right\rangle$ could be calculated in HLA.

So, in distinction from HLA the MB approach within the conventional approximations 1-4, described above, provides the additional factors, collecting information on angular momenta and their projections on the internuclear axis, that could be different in general for various additive terms [5]. However, as it would be demonstrated below *a posteriori* the exact treatment of dependences on angular moments within the MB approach does not give rise to substantial deviations of the broadening coefficients from those obtained within HLA, in particular due to the characteristic power value in the adiabatic theory equal to 2/5 [7]. To be exact this holds at least in the case, when within MB, itemized above, the additional conventional approximations are applied for calculations of atomic polarizabilities.

In the context of above discussion of realistic semi-empirical approximations for calculation of Van der Waals interaction between atoms it is useful to consider atomic pairs containing noble gas atoms. Noble gases are usually employed as bath gases in various mixtures, for instance for filling discharge lamps. In the described conditions the collisions with these atoms usually give the dominant contribution to the broadening of the metal atoms spectral lines. The central part of the spectral profile and to a considerable degree its wings are determined by Van-der-Waals interaction between the colliding atoms. The parameters necessary for the semi-empirical evaluation of Van-der-Waals interaction with Xe and Kr are given in the following table.

Table 2
Electronic Structure Parameters of Kr and Xe

	Kr	*Xe*
Polarizability α_X [a], Å^3	2.5	4.0
Effective excitation energy $\Delta\varepsilon_X$ [b], eV	29.0	25.2

[a] Experimental values tabulated in [20].

[b] Effective excitation energy is estimated basing upon Slater-Kirkwood approximation [5, 24] requiring that calculated in the closure approximation polarizabilities coincide with experimental data.

4. *AB INITIO* ELECTRONIC STRUCTURE MODELING

The *ab initio* electronic structure modeling approaches were used to check the values of $\mathbf{C_6}$ coefficients describing interaction of atoms in the excited states and the perturber atom in the ground state as well as the applicability to approximate the true atom-atom interaction potential by the Van der Waals one.

4.1. Na-Xe Quasi-molecule

Here we consider the results obtained for the Na-Xe quasi-molecule, which could be an excellent example for testing the used approaches. In this case the ground $\mathbf{X^2\Sigma_{1/2}}$ and three lowest excited electronic states $\mathbf{A^2\Pi_{1/2}}$, $\mathbf{A^2\Pi_{3/2}}$, and $\mathbf{B^2\Sigma_{1/2}}$ were considered at internuclear distances R in the range 2.5–10 Å. The employed computational scheme

includes the state-average Complete Active Space Self-Consistent Field (CAS SCF) [40] calculations with single valence electron, and the follow-up account for the dynamic correlation and the spin-orbit coupling effects within the Spin-Orbit Multi-Configurational Quasi-Degenerate 2nd order Perturbation Theory (SO-MCQDPT2) [41]. For both Na and Xe atoms, the shape-consistent effective core potentials (CRENBL) developed by the Christiansen group [42] were used. These effective core potentials allow treating explicitly 2s, 2p and higher shells of Na atom, and 4d, 5s, 5p and higher shells of Xe atom. The AO (atomic orbital) basis set on Na consists of (7s7p5d4f) *uncontracted* Gaussians (*i.e. contractions – the specific linear combinations of Gaussian functions are not used*). This set, developed for the chosen pseudopotential [42], is augmented by few diffuse (*i.e. having smaller exponents*) s- and p-, as well as a set of d- and f- functions. The basis set (5s5p6d2f1g) for Xe was constructed in a similar manner. No significant linear dependency of AO basis set is observed within the range of internuclear separations considered. The calculations were performed using the US GAMESS [43] package of quantum chemical programs. The calculated potential curves of the states $\mathbf{X^2\Sigma_{1/2}}$ and $\mathbf{A^2\Pi_{3/2}}$ are presented in Fig. 2 together with those obtained by fitting the experimental data on the sodium D-line broadening by Xe. It is seen that calculated potential curves agree satisfactorily with those obtained from the experimental data [4].

4.2. Tl-Xe Quasi-molecule

Another interesting example is **Tl-Xe** system. The corresponding data are obtained in the course of quantum-chemical calculations within the basic methodology analogous to that described above for **Na-Xe**, with the only exception that, instead of effective core potential technique, a similar approach based on the model core potentials (**MCP**) was used. The reason for such a modification of the calculation methodology is that model core potentials conserve the correct nodal structure of valence AOs in the core region, thus allowing to properly describe the spin-orbit couplings, what is crucial in the case of rather heavy **Tl** atom. We used the relativistic **MCP** [44] and the associated *segmented* natural-orbital (*i.e. when each Gaussian function appears only in one contraction*) basis sets [45] of **QZP** quality for **Tl** and **Xe** atom, available from [46]. However, in the actual calculations the basis set of **Tl** atom was extended by adding sets of augmentation functions (see Appendix I) to reproduce the relative energy level positions for the thallium atomic states $\mathbf{^2P_{1/2}}$, $\mathbf{^2P_{3/2}}$, $\mathbf{^2S_{1/2}}$, $\mathbf{^2D_{3/2}}$, $\mathbf{^2D_{5/2}}$ within the error of 100-400 cm^{-1} vs the experiment [46]. The calculated data for several states of the Tl-Xe dimer, correlating with certain states of the free **Tl** atom, are presented in Table 3 and Fig. 3.

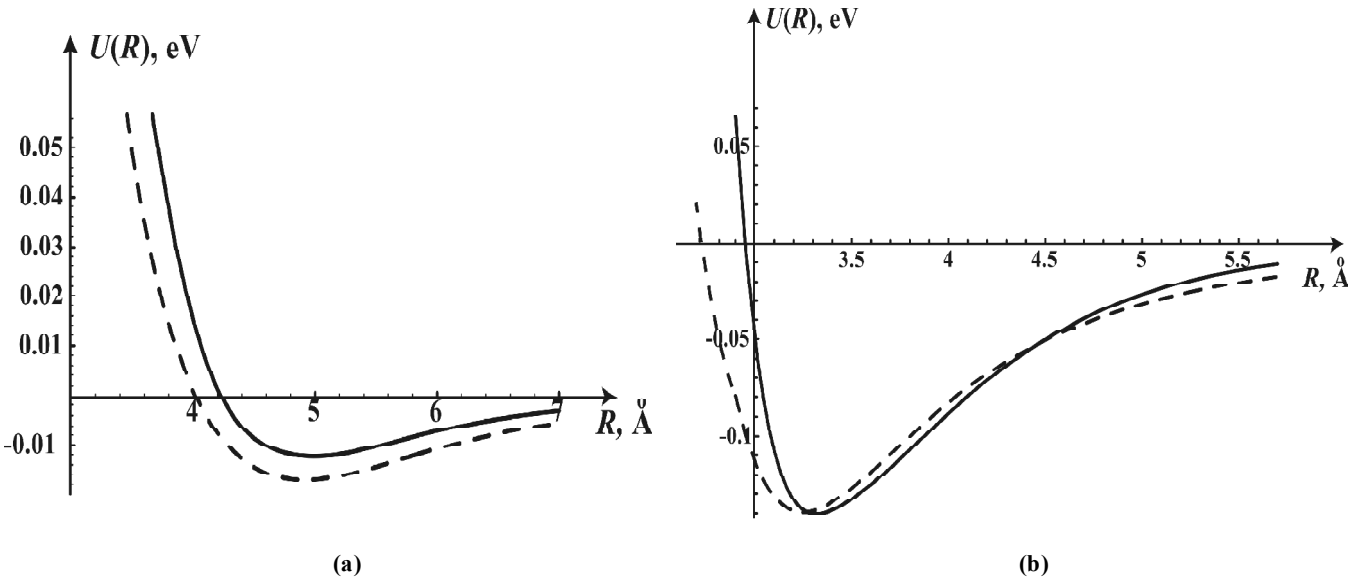

Figure 2: (a) Potential curve of the Na-Xe electronic state $X^2\Sigma_{1/2}$ (solid curve - experiment [4], dashed curve - present quantum chemical calculations); (b) potential curve of the Na-Xe electronic state $A^2\Pi_{3/2}$ (solid curve - experiment [4], dashed curve - present quantum chemical calculations)

Table 3
Data for Tl-Xe Quasimolecule Due to Electron Structure Modeling

Tl-Xe electronic state		*Equilibrium internuclear distance R_e, Å*	*Depth of the potential well D_e, eV*	*Van der Waals coefficient C_6, eV Å^6*
Tl state [a]	Ω [b]			
$6p^1\ ^2P_{1/2}$	½	4.03	0.062	1202
$6p^1\ ^2P_{3/2}$	½	4.80	0.031	1041
	3/2	3.59	0.135	1219
$7s^1\ ^2S_{1/2}$	½	3.31	0.188	2283
$6d^1\ ^2D_{3/2}$	½	3.35	0.260	2083
	3/2	3.35	0.284	3933
	3/2	3.40	0.148	1831
	3/2	3.45	0.173	4760

[a] The state of free Tl atom, with which quasi-molecular Tl-Xe state correlates at infinite internuclear distance,

[b] Ω is absolute value of the projection of the total (orbital +spin) angular momentum on quasi molecular axis

4.3. InXe Quasi-molecule

Ab initio calculations of the potential curves and Van der Waals coefficients $\mathbf{C_6}$ for the **In-Xe** quasi-molecule in 9 electronic states were performed. These states correlate with the lowest **P**, **S** and **D** doublets of free **In** atom originating from single-electronic **5p^1**, **6s^1**, and **5d^1** configurations. The information about these potential curves is necessary for evaluation of the broadening of 5 most intensive **In** spectral lines [12, 39, 47], see Table 4.

The basic methodology used is essentially the same as in the case of Tl-Xe system in the previous subsection 4.2. It includes the Spin-Orbit Many-Configurational Quasi-Degenerated

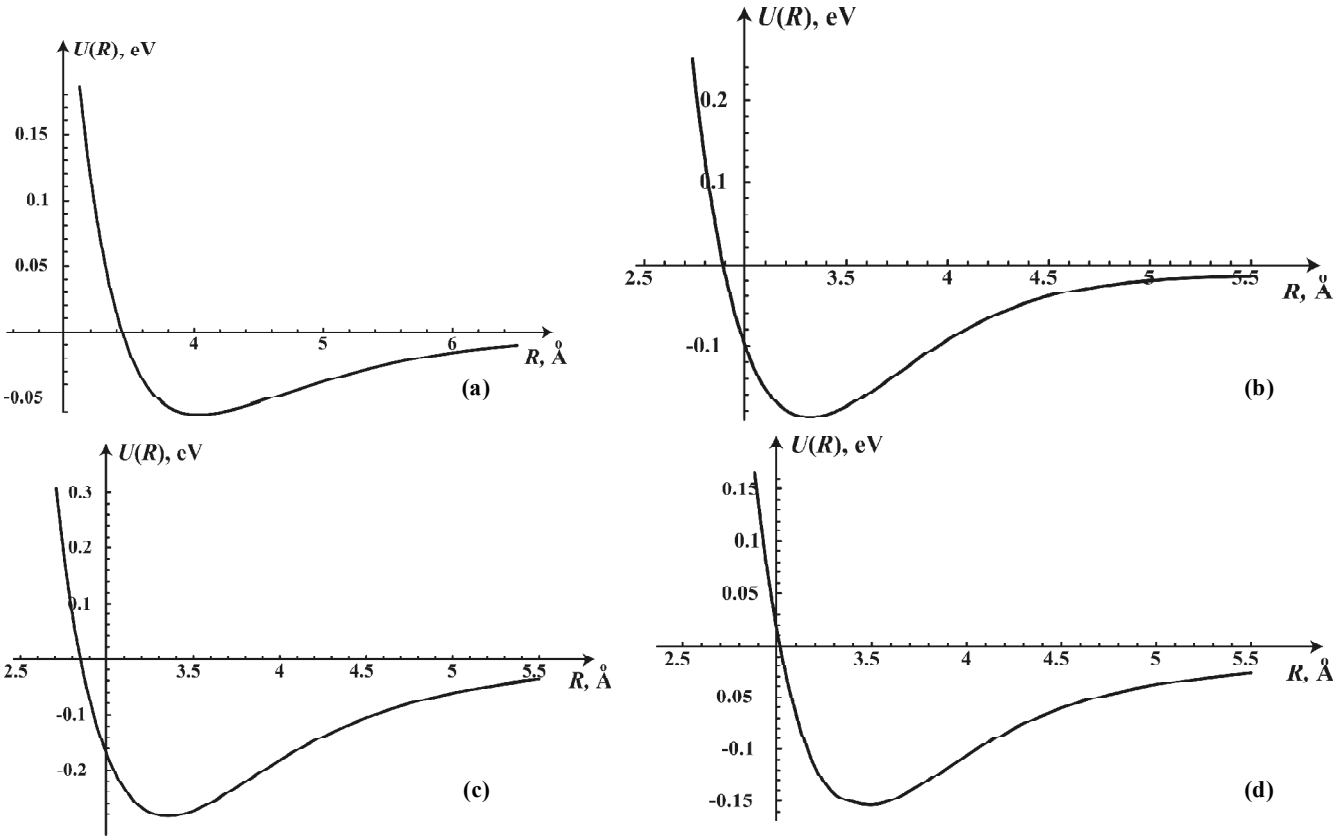

Figure 3: Calculated potential curves of the Tl-Xe electronic states: a – the term with Ω = 1/2, correlating with the ground Tl state $6p^1\ ^2P_{1/2}$; b - the term with Ω = 1/2, correlating with the excited Tl state $7s^1\ ^2S_{1/2}$; c – the term with Ω = 3/2 correlating with the excited Tl state $6d^1\ ^2D_{3/2}$; d – the term with Ω = 1/2 correlating with the excited Tl state $6d^1\ ^2D_5$

Perturbation Theory (SO-MCQDPT) method [41], implemented in the GAMESS US package [43] in combination with a Model Core Potential (MCP) technique [42, 44-46, 48] to reproduce the correct core structure of the valence shells, needed to account for the core-valence correlation and relativistic interactions. The equilibrium distances, depths of potential wells and Van der Waals coefficients $\mathbf{C}_6$ for the calculated potential curves are given in Table 5. The calculated potential curves are used to evaluate the effective difference $\Delta C_{6,if}$ of the Van der Waals coefficients and the profile cutting parameters.

Table 4
Most Intense Radiative Transitions in In [39]

Wavelength (Å)	$A_{ki}(10^8\ s^{-1})$	*Configuration*	*Term*	*J*	*Level* (cm^{-1})
3039.356	1.11	5p	$^2p^o$	1/2	0.000
		5d	^2D	3/2	32892.21
3256.089	1.30	5p	$^2p^o$	3/2	2212.598
		5d	^2D	5/2	32915.54
3258.565	0.30	5p	$^2p^o$	3/2	2212.598
		5d	^2D	3/2	32892.21
4101.7504	0.50	5p	$^2p^o$	1/2	0.000
		6s	^2S	1/2	24372.956
4511.2972	0.89	5p	$^2p^o$	3/2	2212.598
		6s	^2S	1/2	24372.956

Table 5
Parameters of In-Xe potential Curves

In-Xe electronic state		*Equilibrium internuclear distance*	*Depths of the potential wells*	*Van der Waals coefficient*
In state [a]	Ω [b]	R_e, Å	D_e, *eV*	C_6, *eV* × Å^6
$5p^1\ ^2P_{1/2}$	1/2	4.24	0.054	1282
$5p^1\ ^2P_{3/2}$	1/2	3.66	0.098	1370
	3/2	4.8	0.04	1172
$6s^1\ ^2S_{1/2}$	1/2	3.23	0.202	2231
$5d^1\ ^2D_{3/2}$	1/2	3.3	0.273	2422
	3/2	3.3	0.271	1756
	1/2	3.49	0.126	3226
$5d^1\ ^2D_{5/2}$	3/2	3.49	0.117	2130
	5/2	3.31	0.084	1566

[a] State of free **In** atom with which quasi-molecular **In-Xe** state correlates at infinite internuclear distance.

[b] **Ω** is absolute value of the projection of the total (orbital +spin) angular momentum on quasi-molecular axis.

4.4. Nd-X Quasi-molecules in Molecular Basis

4.4.1. Semi-empirical Consideration within MB Approach

In our evaluation of Van der Waals interaction of excited states of atomic Nd, perturbed, for example, by Xe atoms, we evidently need to use fully identified radiative transitions. However, as follows from NIST data [12] there are only few identified radiative transitions in the atomic Nd spectrum. All strong identified radiation lines of Nd correspond to the transition of the electron from the excited 6p-state to the lower 6s-state forming the closed $6s^2$ outer electronic shell of the ground electronic configuration. Data for these transitions from [39] are given in **Table 6**. In **Table 6** "**k**" refers to the upper level and "**i**" to the lower one, $\boldsymbol{A_{ki}}$ is Einstein coefficient, $\mathbf{f_{ik}}$ is oscillator strength, and ***J*** is total electronic angular momentum quantum number.

Table 6
Identified Transitions in Niodymium

Wavelength (Å)	*$A_{ki}(10^8 s^{-1})$ $[f_{ik}]$*	*Configuration*	*Term*	*J*	*Level(cm^{-1})*
4621.94 [b]	0.56	$4f^4 6s^2$	^5I	6	2366.597
	[0.18]	$4f^4 6s6p$	$^5H^o$	6	23996.513
4634.24 [a]	0.84	$4f^4 6s^2$	^5I	4	0.000
	[0.21]	$4f^4 6s6p$	$^5H^o$	3	21572.610
4683.45 [b]	0.52	$4f^4 6s^2$	^5I	4	0.000
	[0.17]	$4f^4 6s6p$	$^5H^o$	4	21345.837
4883.81 [a]	0.88	$4f^4 6s^2$	^5I	8	5048.602
	[0.35]	$4f^4 6s6p$	$^5K^o$	9	25518.700
4896.93 [a]	0.59	$4f^4 6s^2$	^5I	5	1128.056
	[0.25]	$4f^4 6s6p$	$^5K^o$	6	21543.326
4924.53 [a]	0.90	$4f^4 6s^2$	^5I	4	0.000
	[0.40]	$4f^4 6s6p$	$^5K^o$	5	20300.875
4944.83 [c]	0.67	$4f^4 6s^2$	^5I	5	1128.056
	[0.29]	$4f^4 6s6p$	$^5I^o$	6	21345.572
4954.78 [c]	0.29	$4f^4 6s^2$	^5I	4	0.000
	[0.13]	$4f^4 6s6p$	$^5I^o$	5	20176.912

[a] For these transitions both upper and lower states are directly identified.
[b] For these transitions upper state is identified according to its excitation energy.
[c] For these transitions upper state is identified only hypothetically.

The Van-der-Waals interaction between Nd atom in the upper and lower states corresponding to the radiative transition and noble gas atom $X(^1S)$ is determined by the mean square radii for 4f-, 5s-, 5p-, 6s-, and 6p-orbitals, and their effective excitation energies (see, e.g. [5]). These parameters were estimated using the following assumptions: **1**. the relativistic effects can be neglected since only the outer shells of Nd are of interest; **2**. the effective one-electron potential from [16] (it is the other form of GSZ-approximation [16] in atomic units, compare with (2))

$$V(r)=-\frac{2}{r}[(Z-1)S(r)+1], \quad S(r)=\frac{1}{D\,[\exp(r/d)-1]+1}, \quad Z=60,\ D=4.7923,\ d=0.938 \tag{29}$$

can be used to calculate 4f-, 5s-, 5p-, 6s-, and 6p-orbitals of Nd; **3**. the radial atomic orbitals in the potential V(r) can be determined variationally in the basis formed from Coulomb orbitals. The accepted method was verified for atoms with the nuclear charges Z = 40, 50, 70, for which the precise values of one-electron energy levels are available in [16], and has shown sufficient accuracy.

The calculated binding energies for 4f-, 5s-, 5p-, 6s- and 6p-orbitals and corresponding mean square radii are given in Table 5. The Table 5 includes also the average Nd ground state polarizability, calculated in [49] with the use of relativistic linear response method from [50]. This polarizability was used to estimate effective excitation energy of 6s-shell based upon Slater-Kirkwood approximation [5, 24], requiring that calculated in the closure approximation mean polarizability of Nd coincides with the result of calculation in [49].

4.4.2. Van der Waals Interaction between Heavy Noble Gas Atoms X and Nd

As it is known Van der Waals broadening is determined predominantly by those distances between Nd and X, where surely spin-orbit splitting is stronger than interatomic interaction which couples electronic orbital angular momentum to internuclear axis. Therefore spin-orbit coupling is to be taken into account from the beginning (Hund coupling case "**c**" is realized). Having in mind that in Nd **LS** – coupling takes place, Van der Waals interaction constant for the interaction between Nd (**a, JΩ**) and X can be expressed as follows:

Table 7
Electronic Structure Parameters of Nd

	Orbital parameters				
Orbital	*5s*	*5p*	*4f*	*6s*	*6p*
Binding energy, eV	43.03	27.3	17.72	4.97	2.97
Mean square radius $\langle r_{n\ell}^2 \rangle$, Å^2	0.69	0.87	0.28	6.56	12.27
Ground configuration $4f^4 6s^2$ polarizability parameters					
Average polarizability Å^3,				31.4	
Effective $6s^2$-shell average excitation energy $\Delta\varepsilon_{6s}$, eV				4.0	

$$C_{6,J\Omega}^{a} = C_6^{0,a}\left[1 - B_{6,J}^{2,a}\begin{bmatrix} J\ 2\ J \\ \Omega\ 0\ \Omega \end{bmatrix}\right]. \tag{30}$$

Here **"a"** is the set of quantum numbers, identifying configuration and term of **Nd** in the upper or lower states, corresponding to the radiative transition, **Ω** is quantum number of the projection of **Nd** electronic angular momentum on the **Nd-X** quasi-molecule internuclear axis, and $\begin{bmatrix} J\ 2\ J \\ \Omega\ 0\ \Omega \end{bmatrix}$ is the Clebsch-Gordan coefficient. The parameter $B_{6,J}^{2,a}$ in its turn is expressed through the similar parameter $B_6^{2,a}$ entering the expression for the Van der Waals interaction without taking into account spin-orbit coupling (Hund coupling case "**a**"):

$$B_{6,J}^{2,a} = (-1)^{L+S+J}\sqrt{(2L+1)(2J+1)}\begin{Bmatrix} L\ J\ S \\ J\ L\ 2 \end{Bmatrix} B_6^{2,a}, \tag{31}$$

where **L** and **S** are quantum numbers of the total orbital and spin angular momenta of **Nd** and $\begin{Bmatrix} L\ J\ S \\ J\ L\ 2 \end{Bmatrix}$ is 6-j symbol.

The $C_6^{0,a}$ and $B_6^{2,a}$ for the states, corresponding to the upper and lower configurations and terms of **Nd** from **Table 6**, could be expressed within the closure approximation in the form:

upper configuration and terms (Table 6)

$$a\ 5s^2 5p^6 4f^4(^5I)\ 6s\ 6p\ (^1P),\ LS;\ L = 5, 6, 7;\ S = 2, \tag{32}$$

$$C_6^{0,a} = \frac{2\alpha_X\langle r_{5s}^2\rangle\Delta\varepsilon_X}{\Delta\varepsilon_{5s}+\Delta\varepsilon_X} + \frac{6\alpha_X\langle r_{5p}^2\rangle\Delta\varepsilon_X}{\Delta\varepsilon_{5p}+\Delta\varepsilon_X} + \frac{2\alpha_X\langle r_{5s}^2\rangle\Delta\varepsilon_X}{\Delta\varepsilon_{5s}+\Delta\varepsilon_X} + \frac{4\alpha_X\langle r_{4f}^2\rangle\Delta\varepsilon_X}{\Delta\varepsilon_{4f}+\Delta\varepsilon_X} + \frac{\alpha_X\langle r_{6s}^2\rangle\Delta\varepsilon_X}{\Delta\varepsilon_{6s}+\Delta\varepsilon_X} + \frac{\alpha_X\langle r_{6p}^2\rangle\Delta\varepsilon_X}{\Delta\varepsilon_{6p}+\Delta\varepsilon_X}, \tag{33}$$

$$B_6^{2,a} = \frac{1}{C_6^{0,a}}\left[(-1)^{1+L}(2L+1)\sqrt{\frac{6}{5}}\begin{Bmatrix} 1\ L\ 6 \\ L\ 1\ 2 \end{Bmatrix}\frac{\alpha_X\langle r_{6p}^2\rangle\Delta\varepsilon_X}{\Delta\varepsilon_{6p}+\Delta\varepsilon_X} + (-1)^{L}(2L+1)\sqrt{\frac{13}{66}}\sqrt{\frac{28}{15}}\begin{Bmatrix} 6\ L\ L \\ L\ 6\ 2 \end{Bmatrix}\frac{\alpha_X\langle r_{4f}^2\rangle\Delta\varepsilon_X}{\Delta\varepsilon_{4f}+\Delta\varepsilon_X}\right]; \tag{34}$$

lower configuration and terms (Table 6)

$$a = 5s^2\,5p^6\,4f^4(^5I)6s^2(^1S),\ LS;\ L = 6;\ S = 2, \tag{35}$$

$$C_6^{0,a} = \frac{2\alpha_X \left\langle r_{5s}^2 \right\rangle \Delta\varepsilon_X}{\Delta\varepsilon_{5s} + \Delta\varepsilon_X} + \frac{6\alpha_X \left\langle r_{5p}^2 \right\rangle \Delta\varepsilon_X}{\Delta\varepsilon_{5p} + \Delta\varepsilon_X} + \frac{2\alpha_X \left\langle r_{5s}^2 \right\rangle \Delta\varepsilon_X}{\Delta\varepsilon_{5s} + \Delta\varepsilon_X} + \frac{4\alpha_X \left\langle r_{4f}^2 \right\rangle \Delta\varepsilon_X}{\Delta\varepsilon_{4f} + \Delta\varepsilon_X} + \frac{2\alpha_X \left\langle r_{6s}^2 \right\rangle \Delta\varepsilon_X}{\Delta\varepsilon_{6s} + \Delta\varepsilon_X}, \tag{36}$$

$$B_6^{2,a} = -\frac{1}{C_6^{0,a}} \sqrt{\frac{13}{66}} \sqrt{\frac{28}{15(2L+1)}} \frac{\alpha_X \left\langle r_{4f}^2 \right\rangle \Delta\varepsilon_X}{\Delta\varepsilon_{4f} + \Delta\varepsilon_X}. \tag{37}$$

The parameters entering (33), (34), (36), (37) are given in Table 2 and Table 7. For the 4f-, 5s-, 5p-and 6p- shells the effective excitation energies $\Delta\varepsilon_{nl}$ are identified with the binding energies from the Table 7.

4.5. *Ab initio* Calculations of Nd-Xe Potential Curves

4.5.1. Electronic Structure Model and its Validation

At the first glance, high density of electronic states of atomic Nd [39] seems to block the possibility of *ab initio* computing on the intensive 6s-6p transitions in weakly bound diatomics. Indeed, the excited diatomic states of interest will correspond to N^{th} root of electronic Schroedinger equation with N equal to several hundreds, whereas none of existing high-accuracy electronic structure codes can treat more than a few tens of roots. In practice, the possibilities to calculate excited states of diatomics with *f*-elements in a straightforward way are restricted to energies below few (2-5) thousands of wavenumbers [51]. Here we explicitly make use of the following circumstances: no changes in *f*-shell substate occur during intensive excitations of interest [39], in spite of the fact that the changes in *f*-shell occupancies cannot be neglected when treating Nd-containing diatomics with "true" chemical bond. Such neglect seems to be acceptable for weakly bound systems as Nd-Xe, because no f^3-f^4 avoided crossings should be expected to occur at rather large distances. Although the spin-orbit interactions in Nd are not negligible, the potential energy curves of states differing essentially in spin-orbit coupling have nearly identical shape [51].

We used the core pseudopotential based model of Nd-Xe electronic structure with *4f partially filled shell of Nd included in the core*, leaving only the shells with principal quantum number $n \geq 5$ for explicit treatment. This implies the use of different pseudopotentials for f^3 and f^4 states [52-53]. However, this does not give rise to any problem since no intensive transition should connect these states. Only scalar relativistic effects are taken into account; the neglect of spin-orbit interactions reduces dramatically the number of states under treatment. In the present calculations only f^4 subset of states was considered. The model defined by spin-averaged energy-adjusted relativistic pseudopotential [54] for Xe is perfectly consistent with that assumed for neodymium.

In what follows we shall use the term notation corresponding to the electron subsystem comprising the shells $n \geq 5$ of Nd and ignoring the particular substate of the $4f^4$ subshell. For example, atomic term "^{1}S" will correspond to true atomic states $4f^4 6s^2\ ^5I_4$ (ground), $4f^4 6s^2\ ^5I_5$ - $4f^4\ 6s^2\ ^5I_8$, located in the energy range (1128 - 5049 cm^{-1}), and $4f^4 6s^2\ ^5F_1$ - $4f^4 6s^2\ ^5F_5$ in the energy range (10119 - 12895 cm^{-1}) etc. To validate the model, calculations on 6*s*-6*p* like transitions in Nd were performed. The best configuration interaction plus extrapolation and size-consistency correction results are: the excitation energy is 20500 cm^{-1} (cf energies of most intensive 6*s*-6*p* transitions in the Table 8 below), and the transition dipole moment is 3.25 a.u.

The applicability of the model to the description of long-range interactions of *Nd* with **Xe** atom as perturber was estimated through computing *atomic dipole polarizabilities* by the finite-field method, placing a free atom in an uniform electric field (strength F up to 0.008 a.u.) and fitting the dependence of the energy on F by a fourth-order polynomial function (see Fig. 4 for Nd ground state). The polarizability values extracted from the fits along with their experimental counterparts are given in the following Table 9.

Table 8
Energy of Transitions in Nd

Transition	*Transition energy, cm^{-1}*
$4f^4\ 6s^2\ {}^5I_4$ - $4f^4\ 6s\ 6p\ {}^5H_3$	21572.6
$4f^4\ 6s^2\ {}^5I_4$ - $4f^4\ 6s\ 6p\ {}^5K$	20470.1
$4f^4\ 6s^2\ {}^5I_8$ - $4f^4\ 6s\ 6p\ {}^5H_9$	20300.9

Table 9
Comparison of Computed and Experimental Polarizabilities for Nd and Xe

Atom	*computed polarizability*	*experimental polarizability*
Nd	34.2 A^3	31.4 A^3
Xe	3.92 A^3	4.01 A^3

4.5.2. Ab initio Calculations on the NdXe System

Electronic states of the Nd-Xe system correlating with the ground and excited $4f^4 6s6p$ "^1P" states of Nd and Xe ground state were modeled in order to study the long-range behavior of potential energy functions, the relative position of ground and excited state minima and the transition moment variation under changes of the internuclear separation. The following computational scheme was chosen: *accurate singles plus doubles plus perturbative triples coupled cluster (CCSD(T)) ground-state calculations [55];** evaluation of transition moments and estimation of excitation energies as functions of the internuclear distance at the multireference configuration interaction (MRCI) level [56-57] with Siegbahn's size-consistency corrections [58];*** combining the results of (*) and (**) in order to get accurate excited state potential curves (cf. [59]). Basis set superposition errors (BSSE) were carefully eliminated using the counterpoise correction technique [60]. The resulting *potential energy functions* are plotted in Fig. 4. Let us recall that each of these curves in reality corresponds to a large number of states with similar configurations of outer electronic shells and different couplings of *f*-shell angular momenta; the true potential curves for these states should differ only by uniform shifts in energy. "$^1\Pi$-like" states have a smaller equilibrium separation and a stronger binding than the ground state; in contrast, for "$^1\Sigma$-like" excited states a larger equilibrium distance and a weaker bond is observed.

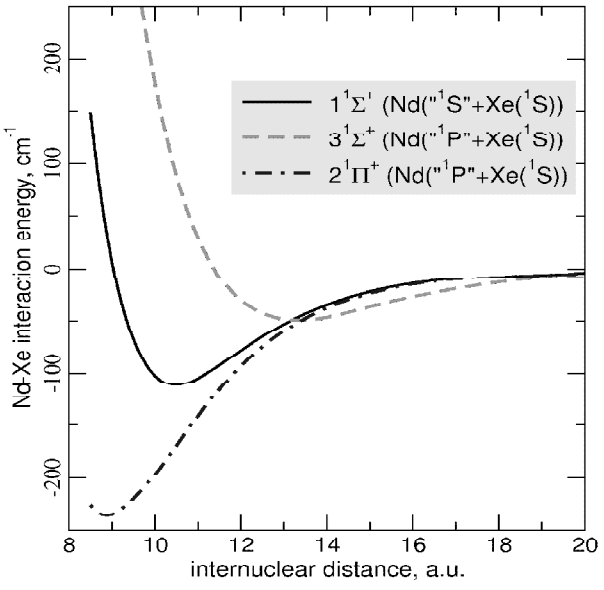

Figure 4: Potential energy functions for ground and excited states of Nd-Xe

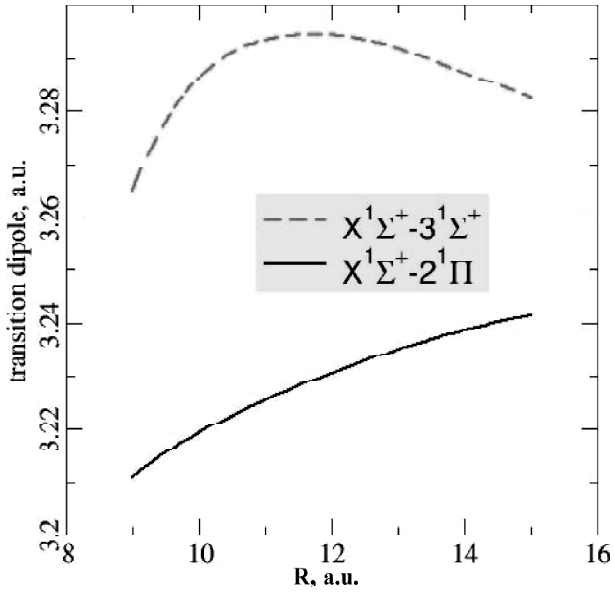

Figure 5: Transition dipoles for 6s-6p excitations in NdXe

The long-range parts of potential energy curves were fitted by C_6/R^6 functions. The main parameters of the curves are summarized in the Table 10.

Table 10
Parameters of Potential Curves of Nd-Xe Quasimolecule

State	*Equilibrium distance, A*	*Dissociation energy, cm^{-1}*	*C_6, a.u.*
$1^1\Sigma^+$ Nd("^{1}S")+Xe(^{1}S)	5.54	111	1135
$3^1\Sigma^+$ Nd("^{1}P")+Xe(^{1}S)	7.07	49	1943
$2^1\Pi$ Nd("^{1}P")+Xe(^{1}S)	4.70	236	1236

Note that the obtained *ab initio* ground-state C_6 value is in an excellent agreement with that obtained by the simplistic London's formula $C_6 = 3\alpha_{Nd}\alpha_{Xe} I_{Nd}I_{Xe}/2(I_{Nd} + I_{Xe}) = 1200$ a.u. (α stands for the polarizability and I for the ionization potential).

The *transition dipole moments* (as functions of the internuclear separation R) between the ground state and excited states arising from $4f^4 6s6p$ "^1P" states of Nd computed by the MRCI [cf. 56-57] method are presented in Fig. 5. The R-dependence of transition moments at R values close to the Van-der-Waals bond length (ca. 10 au) and larger is negligible. Provided that the short-range domain will be of interest, the transition moment lowering at small R might be of importance.

Thus the results of this section show, that modern quantum chemical methods really allow accurately enough calculate potential curves for weakly bound diatomic systems, containing heavy atoms, which are needed for the line broadening calculations, and that modified Buckingham potentials can be used for formulating the explicit procedure of line contour calculations.

As was already pointed out besides the semi-empirical methods used in this work there are now examples of very accurate relativistic calculations of $\boldsymbol{C_6}$ for an excited atom and perturber in the ground states [37-38]. However, firstly those calculations are performed only for a few excited levels and sorts of radiators and perturbers, and secondly their high precision seems to be excessive for the aims of estimations of broadening coefficient evaluation for applied science, as the difference ascribed to employment of these methods could not be distinguished within the accuracy of related experimental measurements. Nevertheless, of course, we do not overestimate the applicability of semi-empirical data, which should be analyzed each time attentively in detail.

5. ATOMIC SPECTRAL LINE BROADENING BY NEUTRAL ATOMS

5.1. Problems in Construction of Total Spectral Line Profile

There are several interrelated problems on the way of construction the total profile of atomic spectral line, resulting due to broadening by neutral atoms [4-5, 7-10, 13-15, 17, 61-65]. Firstly, it should include both impact and quasi-static regions of frequency variation of emitted or absorbed radiation [7-10, 65]. Secondly, it should correctly take into account a quasi-molecular structure of energy levels in compound system of the radiator and perturber pair [5]. The latter in particular is a twofold problem, concerning the influence of the quantum states degeneracy and the behavior of the real interatomic potential versus variation of the distance between radiator and perturber [5, 14-15, 17].

It should be underlined that the rigorous description of Van der Waals broadening for realistic interactions actually could be achieved only in the binary approximation, since even for the interaction of three particles the potential surface becomes too complicated. Thus many-body statistical limit of Van der Waals broadening in fact could not be described accurately even now. Indeed, the many-body statistical limit was constructed starting from Henri Margenau [61] in assumption of scalar additivitity of pairwise contributions from the different perturbers [7], corresponding mainly to operation with scalar terms of Van der Waals interaction, determined by $C_6^{(0,j\gamma)}$. This asymmetric quasi-static profile, derived in [61], has the form

$$I(\Delta\omega_r)=\frac{2\pi N_X\,|\,\Delta C_{6,if}\,|}{\Delta\omega_r^{3/2}}\exp\left(-\frac{4\pi^3}{9}|\,\Delta C_{6,if}\,|\frac{N_X^2}{\Delta\omega_r}\right),\ \Delta C_{6,if}<0,\quad \Delta\omega_r=\omega_{if}-\omega>0,$$
$$I(\Delta\omega_b)=0,\quad \Delta\omega_b=\omega-\omega_{if}>0, \tag{38}$$

where ω is the radiation or absorbing cyclic frequency. If one reminds the spectrally differential criterion of transition from the impact to quasistatic regimes of broadening [7], then at $\Delta\omega_b >> \Omega_W$ (Ω_W is the Weiskopff characteristic frequency [7]) the blue wing of Lorentz symmetric impact profile, proportional to $\Delta\omega_b^{-2}$, in the total line profile vanishes. On the other side of the total line profile the red wing of Lorentz symmetric impact profile, proportional to $\Delta\omega_r^{-2}$, is substituted by the more slowly decreasing quasi-static dependence $\Delta\omega_r^{-3/2}$. In the above consideration we neglect the impact and quasistatic shifts [7], that have values much less than Ω_W. Quite recently to mimic the form of the total profile due to Van der Waals broadening it was proposed to apply the convolution of the Lorentz impact profile with the asymmetric quasi-static profile of Margenau [62]. This is very approximate method as within the considered Van der Waals interaction potential it provides the spurious additional impact broadening contributions in the red and blue line wings at detuning larger than the Weisskopf frequency.

In commonly encountered applications the Van der Waals interaction of metal radiating atoms A (Na, Tl, Sc, Zn etc) and the predominantly noble buffer gas atoms X or sometimes Hg and Zn in the ground ^1S states are of the most practical interest. Thus broadening by buffer gas atoms X in a spherically symmetric ^1S states of the spectral lines of metal atom A, corresponding to the transitions (see Eq. (8)) $A(\gamma_i\, j_i)\rightarrow(\gamma_f\, j_f) + h\nu_0$, has to be evaluated. Here j_i and j_f are the quantum numbers of the total (orbital angular momentum + spin) angular momentum of the radiating atom A in the initial and final states, γ_i and γ_f are sets of all other quantum numbers, characterizing initial and final energy levels, ν_0 is the cyclic frequency of the emitted photon. Always at least one of j_i and j_f is larger than zero for A with even number of electrons or than ½ for A with odd number of electrons. Due to the removal of the degeneracy of the radiating atom state with $j>0$ or ½ by the interaction with the approaching atom X several potential curves of the A–X diatom arise. In particular, several dispersion interactions $\sim 1/R^6$ (R is A–X internuclear distance) exist at large R in this case. Therefore in order to understand possible influence of the appearance of several dispersion interactions explicit expressions for these interactions through the characteristics of $A(\gamma j)$ and $X(^1S)$ are needed.

If to add to above problems additionally nonadiabatic [7-10, 65] interactions, then one could see that the status of the theory of atomic spectral line broadening due to collisions with neutral particles in gases is rather intricate. This statement refers even to the simplest situation of not so high gas densities, when only binary collisions could be taken into account, considering line broadening. There are a number of approaches, models, and approximations in the theory of atomic line broadening by neutrals in the binary approximation. Large efforts were made to get correlations between them (see [8-10, 62-65]), but the situation still remains quite complicated. That is why the reliable data should be generated by the most simple and universal way, chosen to evaluate and parameterize line contours, based upon existing theoretical methods.

So, in the case under consideration for the construction of total line contour in binary approximation with account of degeneracy it is necessary firstly to clarify the form of A-X interaction potential and to make choice of the most suitable analytical approximation, that would correspond to this form. Luckily, the binary approximation is advantageous due to possibility to apply Unified Theory approaches [8, 14-15], that provide the line profile, including impact and statistical regions, as well as possible existing satellites. As with account of degeneracy with the existence of several dispersion interactions $\mathbf{\sim 1/R^6}$ at large distances it is necessary to find how these several interaction potentials could be taken into account for one spectral line.

Another known problem of the total profile concerns its behavior in the wings. It is directly linked with the choice of interaction potential. The dispersion type of potential becomes inappropriate at sufficiently small distances, for instance, much less than the location of minimum of real potential. So, at the sufficiently large frequency detuning from the line center the power type frequency dependence of profile in the wings should be substituted by the exponential drop due to repulsion (see e.g.[5]). As the calculations with a real potential are much more complicated

it is widely used to implement the dispersion potential for profile calculations, for instance, for absorption coefficients. At the same time the adequate cutting procedures of profile wings to amend its behavior with account of repulsive part of the real potential at large detunings from the line center is introduced. The only way to consider this rather rigorously is to study the behavior in the wings in the binary approximation within Unified Theory [14-15, 68], and basing on it, to elaborate reasonable, physically grounded and general recommendations for cutting procedures of the far wings. In particular this allows to reduce significantly computation time, which considerably increases under attempts to take into account spurious contributions, proportional to $1/\Delta\omega^{3/2}$ and $1/\Delta\omega^2$. At the end, it is worthy to note that the Van der Waals broadening usually could be considered in the binary approximation even for rather high densities of perturbers due to the fulfillment of integral criterion [7], which is expressed in the form of inequality

$$h_{Van\ der\ Waals} = N_X \rho_W^{\ 3} << 1,$$

where ρ_W is the Weisskopf radius for Van der Waals interaction, determined for the mean value of relative thermal velocity of radiator and perturber $\langle u \rangle = (8k_BT/\pi\mu)^{1/2}$ (μ being reduced mass of A-X pair) in the form

$$\rho_w = \left(\frac{\Delta C_{6,if}}{\left(8k_BT/\pi\mu\right)^{1/2}} \right)^{\frac{2}{5}}, \Delta C_{6if} = |C_{6,i} - C_{6,f}|.$$

Thus, this supports the implementation of UFCT. Below we shall consider pointed above problems gradually.

5.2. Impact Van der Waals broadening with Account of Degeneracy

In the present section the impact limit of the total line contour [7] will be considered, and by its direct derivation the methodology of degeneracy treating will be demonstrated.

The impact width of the radiation line corresponding to the dipole transition (8) is determined by the relaxation of non-diagonal irreducible matrix elements of the atom A density matrix $\rho^{1q}_{\gamma_i j_i;\gamma_f j_f}$. The corresponding relaxation cross section could be expressed through the elements of the A – X scattering matrix in the form (see [5, 13])

$$\sigma^{(1)}_{\gamma_i j_i;\gamma_f j_f}(\varepsilon_t) = \mathrm{Re}\left\{ \frac{\pi}{k^2} \sum_{J_i J_f} \sum_{ll'} (-1)^{l-l'} (2J_i+1)(2J_f+1) \begin{Bmatrix} J_f & J_i & 1 \\ j_i & j_f & l \end{Bmatrix} \times \right.$$
$$\left. \times \begin{Bmatrix} J_f & J_i & 1 \\ j_i & j_f & l' \end{Bmatrix} \left[\delta_{ll'} - S^{J_i,\gamma_i j_i}_{l';l}(\varepsilon_t) S^{J_f,\gamma_f j_f}_{l';l}(\varepsilon_t) \right] \right\}. \quad (39)$$

Here $\hbar J_i$, $\hbar J_f$ are total (electronic + nuclear) angular momenta of the diatom A–X, $\hbar l$, $\hbar l'$ are angular momenta of the relative motion of A and X, k is the wave number of the relative motion of A and X at infinite separation, $S^{J_i,\gamma_i j_i}_{l';l}(\varepsilon_t)$ and $S^{J_f,\gamma_f j_f}_{l';l}(\varepsilon_t)$ are scattering matrix elements for A($\gamma_i j_i$)–X and A($\gamma_f j_f$)–X collisions at relative kinetic energy

$$\varepsilon_t = \frac{\hbar^2 k^2}{2\mu}, \quad (40)$$

and μ is the A–X reduced mass. It is to be noted that the processes involved in impact line broadening which are described by the scattering matrices $S^{J_i,\gamma_i j_i}_{l';l}$ and $S^{J_f,\gamma_f j_f}_{l';l}$ are resonance in that sense that internal energy of atom A is not changed. Elastic scattering and scattering accompanied by the change of electronic angular momentum of A change its direction in space (depolarization).

Eq. (39) can be simplified considerably taking into account that the main contribution to the sum over J_i, J_f is given by

$$J_i, J_f >> 1 \tag{41}$$

On the other hand

$$j_i, j_f \sim 1 \tag{42}$$

and therefore ℓ, ℓ' may differ from J_i, J_f by the value of the order of 1, and the difference between J_i and J_f is also of the order of 1. Having this in mind it is suitable to introduce (see [5]) new summation variables in (39)

$$J = (J_i + J_f)/2; \rho = J_i - J_f; m = J_i - \ell; m' = J_i - \ell' \tag{43}$$

Doing this it is suitable to set

$$S^{J_i,\gamma_i j_i}_{l';l} = \exp\left[-\frac{i\pi}{2}(3m - m')\right] S^{J+(\rho/2),\gamma_i j_i}_{m';m} \tag{44}$$

$$S^{J_f,\gamma_f j_f}_{l';l} = \exp\left[-\frac{i\pi}{2}(3m - m') + i\pi\rho\right] S^{J-(\rho/2),\gamma_f j_f}_{m'-\rho;m-\rho} \tag{45}$$

Then having in mind that $J >> 1$ and using asymptotic expression for 6-j symbols (see, e.g. [66]), the following simplified expression for the broadening cross section $\sigma^1_{\gamma_i j_i;\gamma_f j_f}(\varepsilon_t)$ is obtained

$$\begin{aligned}\sigma^{(1)}_{\gamma_i j_i;\gamma_f j_f}(\varepsilon_t) = \mathrm{Re}\Bigg\{\frac{\pi}{k^2}\sum_J 2J \sum_{mm'\rho}\frac{1}{3}(-1)^{m-m'}\begin{bmatrix} j_i & j_f & 1 \\ m & \rho\text{-}m & m\end{bmatrix}\begin{bmatrix} j_i & j_f & 1 \\ m' & \rho\text{-}m' & m'\end{bmatrix}\times \\ \times\left[\delta_{mm'} - \exp(-i\pi\rho) S^{J+(\rho/2),\gamma_i j_i}_{m';m}(\varepsilon_t) S^{J-(\rho/2),\gamma_f j_f}_{m'-\rho;m-\rho}(\varepsilon_t)\right]\Bigg\}.\end{aligned} \tag{46}$$

Scattering matrix is obtained solving the system of radial scattering equations (see [5])

$$\begin{aligned}\left[-\frac{\hbar^2}{2\mu}\frac{d^2}{dR^2} + \frac{\hbar^2(J+1/2)^2}{2\mu R^2} - \varepsilon_t\right]\eta^{J,\gamma j}_{m';m}(R) = \\ = -\sum_{m''}\left(\left\langle \gamma j m'\middle| V^{(d)}(R)\middle| m'' j\gamma\right\rangle - \frac{\hbar^2(J+1/2)m''}{\mu R^2}\delta_{m'm''}\right)\eta^{J,\gamma j}_{m'';m}(R),\end{aligned} \tag{47}$$

with the following boundary conditions

$$\eta^{J,\gamma j}_{m';m}(R) \underset{R\to 0}{\to} 0, \tag{48}$$

$$\eta^{J,\gamma j}_{m';m}(R) \underset{R\to\infty}{\to} k^{-1/2}\left\{\exp[-i(kR - J\pi/2)]\delta_{mm'} - S^{J,\gamma j}_{m';m}\exp[i(kR - J\pi/2)]\right\}. \tag{49}$$

Here $\left\langle \gamma j m'\middle| V^{(d)}(R)\middle| m'' j\gamma\right\rangle$ are matrix elements between the wave functions $\left|mj\gamma\right\rangle$ of the atom A of the dispersion interaction. The quantities $\hbar m$, $\hbar m'$ are the projections of the atom A electronic angular momentum upon the axis z_1 along the total (electronic + nuclear) angular momentum of the diatom A–X, see Fig. 6. The axis $\boldsymbol{z_1}$ is normal to the A–X collision plane (plane $\boldsymbol{x_1 y_1}$, see Fig. 6).

Reference frame $\boldsymbol{x_1 y_1 z_1}$ is obtained from the coordinate frame $\boldsymbol{x y z}$ presented in Fig. 1 by the rotation with the Euler angles (see [5]) $\boldsymbol{\alpha = 0}$, $\boldsymbol{\beta = \pi/2}$, $\boldsymbol{\gamma = \pi}$. Therefore matrix elements $\left\langle \gamma j m'\middle| V^{(d)}(R)\middle| m'' j\gamma\right\rangle$ are expressed through the parameters determining $V^{(d)}_{\gamma j\tilde{\Omega}}(R)$ (see (24)) as follows

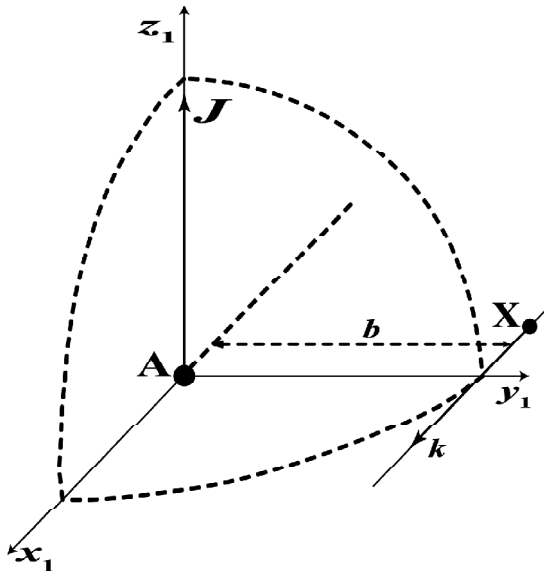

Figure 6: Reference frame in which A-X collision is considered

$$\left\langle \gamma j m' \left| V^{(d)}(R) \right| m'' j\gamma \right\rangle = -\frac{C_6^{(0,j\gamma)}}{R^6}\left[\delta_{m'm''} - B_6^{(2,j\gamma)} F(j,m',m'')\right], \tag{50}$$

$$F(j,m',m'') = \sum_{\tilde{\Omega}=-j}^{j} D^{j}_{\tilde{\Omega}m'}(0,\pi/2,\pi) * \begin{bmatrix} j & 2 & j \\ \tilde{\Omega} & 0 & \tilde{\Omega} \end{bmatrix} D^{j}_{\tilde{\Omega}m''}(0,\pi/2,\pi) \tag{51}$$

Here $D^{j}_{\tilde{\Omega}m}(\alpha,\beta,\gamma)$ are Wigner rotation matrices (see [67]).

Under the conditions typical for the impact broadening of radiation lines of the metal atoms (the resonant character of collision process and high temperatures) the scattering matrix $S^{J,\gamma j}_{m';m}$ can be determined in the framework of following approximations: 1. scattering equations (47) can be solved in the common-trajectory (semiclassical) approximation (see [5]), in which it is assumed that the relative motion of A and X takes place along the classical trajectory $R(t)$, where t is time; 2. the trajectory of the relative A and X motion is rectilinear (impact parameter method) and therefore

$$R(t) = \sqrt{b^2 + u^2 t^2}\ , \tag{52}$$

where $u = \hbar k/\mu$ is the relative velocity of A and X motion at infinity and $\boldsymbol{b}$ is an impact parameter (see Fig. 6).

Under these assumptions the scattering matrix is obtained within the following steps. Firstly the set of second order scattering equations (47) is reduced to the set of first order equations

$$i\hbar \frac{d}{dt} c^{b,\gamma j}_{m';m}(t) = $$
$$= -\sum_{\nu''}\left(\left\langle \gamma j m' \left| V^{(d)}[R(t)] \right| m'' j\gamma \right\rangle - \frac{\hbar b u m''}{R(t)^2}\delta_{m'm''} \right) c^{b,\gamma j}_{m'';m}(t). \tag{53}$$

These equations are solved with the initial conditions

$$c^{b,\gamma j}_{m';m}(t) \underset{t\to-\infty}{\to} \delta_{m'm} \tag{54}$$

Deriving (49) it was taken into account that

$$\hbar \boldsymbol{J} = \boldsymbol{\mu u b}. \tag{55}$$

The scattering matrix $S^{\gamma j}_{m';m}(b) = S^{J;\gamma j}_{m';m}$ (relation (55) is taken into account) is determined by the solution of the equations (53-54)

$$S^{\gamma j}_{m';m}(b) = c^{b,\gamma j}_{m';m}(t \to \infty). \tag{56}$$

Taking into account of (55) and mentioned above fact that the main contribution to the broadening cross section is given by collisions with large $\boldsymbol{J}$ (large $\boldsymbol{b}$) the sum (46) may be transformed to the integral over $\boldsymbol{b}$

$$\sigma^{(1)}_{\gamma_i j_i;\gamma_f j_f}(\varepsilon_t) = \mathrm{Re}\left\{ 2\pi \int_0^\infty b db \sum_{mm'\rho} \frac{1}{3}(-1)^{m-m'} \begin{bmatrix} j_i & j_f & 1 \\ m & \rho\text{-}m & m \end{bmatrix} \begin{bmatrix} j_i & j_f & 1 \\ m' & \rho\text{-}m' & m' \end{bmatrix} \times \right.$$
$$\left. \times \left[\delta_{mm'} - \exp(-i\pi\rho) S^{\gamma_i j_i}_{m';m}(b) S^{\gamma_f j_f}_{m'-\rho;m-\rho}(b) \right] \right\}. \tag{57}$$

The difference between $S^{J\pm(\rho/2),\gamma j}_{m';m}$ and $S^{J,\gamma j}_{m';m}$ is neglected in (57) (compare with (46)) due to the assumption 2, because for the rectilinear trajectory, the deflection function is zero (see the discussion of this point in [5]).

Equations (53) can not be solved analytically. However, to get transparent correlation between the scattering matrix and dispersion interaction parameters $C_6^{(0,j\gamma)}$ and $B_6^{(2,j\gamma)}$ some approximation have to be made. The adequate approximation could be developed if several specific features of the problem will be taken into account. Firstly, it can be readily shown that determined by (51) function $F(j, m', m'') = 0$ if $m'\text{-}m''$ is odd. Secondly, the impact broadening is determined by those impact parameters at which imposed by collision with X the phase shift $\delta_m^{(j\gamma)}(b)$ of the atom A electronic wave function $|mj\gamma\rangle$ is of the order of unity

$$\left|\delta_m^{(j\gamma)}(b)\right| \approx \left| \frac{1}{\hbar} \int_{-\infty}^{\infty} \langle \gamma jm | V^{(d)}[R(t)] | mj\gamma \rangle dt \right| \sim 1 \tag{58}$$

Thirdly, at such impact parameters inequality holds

$$\left| \frac{1}{\hbar} \int_{-\infty}^{\infty} \langle \gamma jm | V^{(d)}[R(t)] | (m \pm 2)\, j\gamma \rangle dt \right| < \left|\delta_m^{(j\gamma)}(b)\right| < 1, \tag{59}$$

because always

$$\left| B_6^{(2,j\gamma)} F(j, m', m'') \right| < 1. \tag{60}$$

Fourthly, it could be shown, that if $R(t)$ is given by (52) then

$$\int_{-\infty}^{\infty} \frac{bum}{R(t)^2} dt = \pi m, \tag{61}$$

and therefore, having also in mind (58-59), the following inequalities take place

$$\left| \frac{1}{\hbar} \int_{-\infty}^{\infty} \langle \gamma jm | V^{(d)}[R(t)] | m \pm 2\, j\gamma \rangle dt \right| \ll \left| \int_{-\infty}^{\infty} dt \left[\frac{1}{\hbar} \left(\langle \gamma jm | V^{(d)}[R(t)] | mj\gamma \rangle - \right. \right. \right.$$
$$\left. \left. \left. - \langle \gamma j(m \pm 2) | V^{(d)}[R(t)] | (m \pm 2)\, j\gamma \rangle \right) - \left(\frac{bum}{R(t)^2} - \frac{bu(m \pm 2)}{R(t)^2} \right) \right] \right| \approx 2\pi. \tag{62}$$

Inequality (62) means (see [5]) that the effect of coupling between the states with different m in equations (53), induced by nondiagonal matrix elements $\langle \gamma j m' | V^{(d)}[R(t)] | (m' \pm 2) j \gamma \rangle$ is small. Hence the reasonable approximation should neglect such coupling. In this approximation the scattering matrix, obtained solving equations (53), has the form

$$S^{\gamma j}_{m';m}(b) = \delta_{m'm} \exp\left[-iW^{\gamma j}_{m}(b)\right], \tag{63}$$

where

$$\begin{aligned} W^{\gamma j}_{m}(b) &= \int_{-\infty}^{\infty} \left\{ -\frac{bum}{R(t)^2} - \frac{C_6^{(0,j\gamma)}}{\hbar R(t)^6} \left[1 - B_6^{(2,j\gamma)} F(j,m,m) \right] \right\} dt = \\ &= -\pi m - \frac{3\pi}{8} \frac{C_6^{(0,j\gamma)}}{\hbar b^5 u} \left[1 - B_6^{(2,j\gamma)} F(j,m,m) \right]. \end{aligned} \tag{64}$$

Substituting expressions (63), (64) for $S^{\gamma_i j_i}_{m';m}(b)$ and $S^{\gamma_f j_f}_{m'-\rho;m-\rho}(b)$ in (57) the following expression for $\sigma^{(1)}_{\gamma_i j_i;\gamma_f j_f}(\varepsilon_t)$ is obtained

$$\sigma^{(1)}_{\gamma_i j_i;\gamma_f j_f}(\varepsilon_t) = 2\pi \int_0^{\infty} b\, db \sum_{m,\rho} \frac{1}{3} \begin{bmatrix} j_i & j_f & 1 \\ m & \rho\text{-}m & m \end{bmatrix}^2 \times \left\{ 1\text{-}\cos\left[\frac{3\pi \left(C_6^{(0,j_i\gamma_i)} - C_6^{(0,j_f\gamma_f)} \right)}{8\hbar b^5 u} \Gamma^{(j_i\gamma_i;j_f\gamma_f)}_{m;\rho} \right] \right\}, \tag{65}$$

where

$$\Gamma^{(j_i\gamma_i;j_f\gamma_f)}_{m;\rho} = 1 + \frac{1}{C_6^{(0,j_i\gamma_i)} - C_6^{(0,j_f\gamma_f)}} \left[C_6^{(0,j_f\gamma_f)} B_6^{(2,j_f\gamma_f)} F(j_f, m-\rho, m-\rho) - C_6^{(0,j_i\gamma_i)} B_6^{(2,j_i\gamma_i)} F(j_i,m,m) \right]. \tag{66}$$

Calculating integrals in (65) over "b", one can arrive to the following final expression for $\sigma^{1}_{\gamma_i j_i;\gamma_f j_f}(\varepsilon_t)$

$$\begin{aligned} \sigma^{(1)}_{\gamma_i j_i;\gamma_f j_f}(\varepsilon_t) &= \frac{1}{8 \times 2^{1/5}} \left[3^{2/5} (1+\sqrt{5}) \pi^{7/5} \Gamma(3/5) \right] \left[\frac{\Delta C^{(imp)}_{6,eff}(\gamma_i j_i;\gamma_f j_f)}{\hbar u} \right]^{2/5} = \\ &= 4.041 \left[\frac{\Delta C^{(imp)}_{6,eff}(\gamma_i j_i;\gamma_f j_f)}{\hbar u} \right]^{2/5}, \end{aligned} \tag{67}$$

where

$$\Delta C^{(imp)}_{6,eff}(\gamma_i j_i;\gamma_f j_f) = \left| C_6^{(0,j_i\gamma_i)} - C_6^{(0,j_f\gamma_f)} \right| \left[\sum_{m\rho} \frac{1}{3} \begin{bmatrix} j_i & j_f & 1 \\ m & \rho\text{-}m & m \end{bmatrix}^2 \left| \Gamma^{(j_i\gamma_i;j_f\gamma_f)}_{m;\rho} \right|^{2/5} \right]^{5/2}. \tag{68}$$

The impact broadening halfwidth $\Delta\nu_{1/2}(j_i\gamma_i; j_f\gamma_f)$ of the spectral line corresponding to the transition (8) is expressed through the cross section $\sigma^{(1)}_{\gamma_i j_i;\gamma_f j_f}(\varepsilon_t)$ as follows

$$\Delta\nu_{1/2}(j_i\gamma_i; j_f\gamma_f) = N_X \left\langle u\, \sigma^{(1)}_{\gamma_i j_i;\gamma_f j_f} \right\rangle / (2\pi), \tag{69}$$

where N_X is the density of the bath gas X,

$$\langle u \rangle = \sqrt{\frac{8k_B T}{\pi \mu}} \tag{70}$$

is the average relative velocity of X with respect to A at temperature T, and

$$\begin{aligned} \left\langle u \sigma^{(1)}_{\gamma_i j_i;\gamma_f j_f} \right\rangle &= \langle u \rangle \int_0^\infty \frac{\varepsilon_t d\varepsilon_t}{(k_B T)^2} \sigma^{(1)}_{\gamma_i j_i;\gamma_f j_f}(\varepsilon_t) \exp\left(-\frac{\varepsilon_t}{k_B T}\right) = \\ &= \frac{1}{8 \times 2^{1/5}} \left[3^{2/5}(1+\sqrt{5})\pi^{7/5}\Gamma(3/5)\right](4/\pi)^{1/5}\Gamma(9/5)\langle u \rangle \left[\frac{\Delta C^{(imp)}_{6,eff}(\gamma_i j_i;\gamma_f j_f)}{\hbar \langle u \rangle}\right]^{2/5} = \\ &= 3.95 \langle u \rangle \left[\frac{\Delta C^{(imp)}_{6,eff}(\gamma_i j_i;\gamma_f j_f)}{\hbar \langle u \rangle}\right]^{2/5}. \end{aligned} \tag{71}$$

is the thermally averaged broadening rate. If the line profile is considered as a function of the wavelength $\lambda = c/\nu$ ($\lambda_0 = c / \nu_0$, c is speed of light), but not the frequency ν, the corresponding halfwidth $\Delta\lambda_{1/2}(j_i, \gamma_i; j_f\gamma_f)$ is given by the following expression

$$\Delta\lambda_{1/2}(j_i\gamma_i; j_f\gamma_f) = 3.95\ N_X \langle u \rangle^{3/5} \frac{\lambda_0^2}{2\pi c} \left[\frac{\Delta C^{(imp)}_{6,eff}(\gamma_i j_i;\gamma_f j_f)}{\hbar}\right]^{2/5}, \tag{72}$$

or in the cyclic frequency scale this equation could be readily rewritten as

$$\Delta\omega^{(imp)}_{1/2} = 3.9504\, N_X \cdot \langle u \rangle \left(\frac{\Delta C^{(imp)}_{6,eff}}{\hbar \langle u \rangle}\right)^{2/5}. \tag{73}$$

It is worthy to note, that the numerical coefficient **3.9504** in (73) corresponds to averaging over Maxwell distribution, while the simple substitution of the relative A-X velocity u by the average relative A-X velocity $\langle u \rangle$ leads to the numerical coefficient 4.04.

Thus the obtained result for general standard expression for $\Delta\omega_{1/2}$ via the A-X scattering matrix elements (see, e.g. [13]) consistently resolves the problem of electronic degeneracy. It describes the impact core of the Lorentz unified profile due to the A-X collision processes in which internal energy of atom A is not changed. These processes are the elastic A-X scattering and the scattering accompanied by the change of the direction in space of the electronic angular momentum of A (depolarization). The collisional broadening cross section, which determines the Lorentz core of the line is governed predominantly by the distant collisions between A and X. At these interatomic distances the Coriolis interaction $\sim 1/R^2$ is higher in absolute value than the splitting between different molecular terms, arising due to the Van der Waals interaction between A(j) (with j > 0 or ½) with X. That is why the adiabatic approach to the description of Van der Waals broadening is quite adequate, as well as the assumption of the rectilinear trajectories of relative A and X motion and implementation of the quasiclassical theory of atomic collisions (see [5]). The quantity $\Delta C_{6,eff}$ is expressed explicitly through characteristics of $A(j_i)$, $A(j_f)$ (average squares of electron distance from the nuclear, ionization potentials), polarizability of X and tabulated functions of the theory of quantum angular momentum. As it could be seen this result is typical in its settings for the collision theory as information about projections of angular momentum quantum numbers is wiped out due to the summation over the initial projections and average over the final ones in definition of (68).

For the illustration of developed theory the $\Delta C_{6,\mathrm{eff}}^{(\mathrm{imp})}$ value was evaluated for the impact broadening by **Xe** and Zn of four strong Tl lines. The results are presented in Table 11. It is seen that the values $\Delta C_{6,\mathrm{eff}}^{(\mathrm{imp})}$, corresponding to transitions either from the different components of upper states multiplet to one of the lower states or from the upper state to the different components of lower state multiplet differ slightly. Having in mind that $\Delta C_{6,\mathrm{eff}}^{(\mathrm{imp})}$ enters the expression for the line width in the power 2/5 (see (67)), it could be concluded from the practical point of view that the accurate treating of depolarization of degenerate atomic states of A by X at large impact parameters is immaterial. In particular the purely electronically adiabatic treatment of atomic collision neglecting the Coriolis coupling can be used considering line broadening. This conclusion is important since purely adiabatic picture of atomic collision is the corner stone of the Unified Franck-Condon Theory (UFCT) of line broadening [8, 14-15], which provides a quite accurate procedure for evaluating the entire line contour in the binary approximation.

Table 11
Strong Tl lines, Einstein Coefficients and Effective Differences of Constants of Dispersion Interactions for Collisions with Xe and Zn

Transition	*Wavelength, nm*	*Einstein coefficient* A_{if}, $10^8\ s^{-1}$	$\Delta C_{6,\mathrm{eff}}^{(\mathrm{imp})}$, $eV \times Å^6$	
			X=Xe	*X=Zn*
$6s^26d(^2D_{5/2}) \rightarrow 6s^26p(^2P_{3/2})$	351.924	1.24	1443	2351
$6s^26d(^2D_{3/2}) \rightarrow 6s^26p(^2P_{3/2})$	352.943	0.22	1443	2352
$6s^27s(^2S_{1/2}) \rightarrow 6s^26p(^2P_{1/2})$	377.572	0.625	451	689
$6s^27s(^2S_{1/2}) \rightarrow 6s^26p(^2P_{3/2})$	535.046	0.795	-411	631

In its turn the effective differences of the Nd-X Van-der-Waals interaction constants in the upper and lower states of Nd for all radiative transitions from Table 6, are calculated using (30-37), (68) and data from Tables 2 and 7, and given in Table 12 for two sorts of perturbers Kr and Xe.

Table 12
Effective Differences $\Delta C_{6,eff}$ of Nd-X Van-der-Waals Interaction Constants, which Determine Broadening of Strong Nd Radiation Lines

Transition	*Wavelength,Å*	$\Delta C_{6,eff}$; *X=Kr,a.u.* $(eV \times Å^6)$	$\Delta C_{6,eff}$; *X=Xe,* *a.u.*$(eV \times Å^6)$
$4f^46s6p(^5H_6)$	4621.94	312.1	492.6
$4f^46s^2(^5I_6)$		(186.6)	(294.3)
$4f^46s6p(^5H_3)$	4634.24	311.4	492.1
$4f^46s^2(^5I_4)$		(186.1)	(294.0)
$4f^46s6p(^5H_4)$	4683.45	312.2	493.3
$4f^46s^2(^5I_4)$		(186.5)	(294.8)
$4f^46s6p(^5K_9)$	4883.81	301.	476.5
$4f^46s^2(^5I_8)$		(180.2)	(284.6)
$4f^46s6p(^5K_6)$	4896.93	304.3	480.7
$4f^46s^2(^5I_5)$		(181.8)	(287.2)
$4f^46s6p(^5K_5)$	4924.53	302.3	477.6
$4f^46s^2(^5I_4)$		(180.6)	(285.3)
$4f^46s6p(^5I_6)$	4944.83	277.6	438.1
$4f^46s^2(^5I_5)$		(166.0)	(262.0)
$4f^46s6p(^5I_5)$	4954.78	278.5	439.6
$4f^46s^2(^5I_4)$		(166.5)	(262.9)

The data in Table 12 allows to conclude that calculated values of $\Delta C_{6,\text{eff}}$ practically completely (within the range of about 12%) are determined by electronic configurations of the upper and lower states of the Nd radiating atoms. This supports *ab initio* quantum chemical calculations approach which neglects the degeneracy of $4f^4$- shell states of Nd and spin-orbit interaction.

5.3. Analytical Modified Buckingam Potential

The interaction potentials $U(R)$ (R is internuclear distance) of metal atoms A in the ground and excited states with the bath atoms X in the ground spherically symmetric ^1S states were studied in detail both experimentally and theoretically [4-5, 8, 68 -70]. These potentials have several general properties (see Fig. 7). Firstly, at small enough R the interaction potential is strongly repulsive - $U(R) \propto \exp(-\alpha R)$ - and depends exponentially on R. Secondly, at intermediate distances the rather shallow Van der Waals potential well exists with the depth D_e at equilibrium distance R_e. And thirdly, at large enough distances the dispersion attraction takes place $U(R) = -C_6/R^6$.

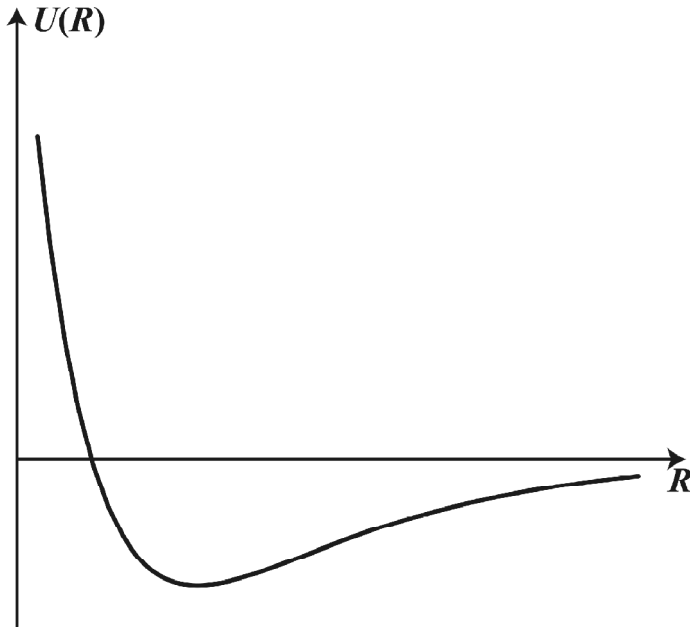

Figure 7: Qualitative form of the A-X interaction potential

The investigations of several interaction potentials of alkali atoms with noble gas atoms or Hg have shown that reasonable approximation to the A-X interaction potential can be obtained using modified Buckingam potential

$$U_{\text{B}}(R) = A\exp(-\alpha R) - \frac{C_6}{(R^2 + R_0^2)^3} \tag{74}$$

In (74) the Van der Waals constant C_6 is either calculated by some approximate method or determined by fitting the tail of quantum-chemical or experimental interaction potential. The parameter α is obtained by approximating by an exponential function the repulsive part of the potential calculated quantum chemically or determined experimentally. The two remaining parameters A and R_0 are determined by fitting the potential curve, obtained experimentally or from quantum chemistry, in the region of the potential well. It is to be noted that the real potentials which could describe all the details of the line contour could be much more complicated than (74). But for understanding the contribution of different regions of R variation into the line profile it is sufficient to consider this rather simple four-parameter form.

For example, the potential curves of the Na-Xe system (both calculated and experimental) could be accurately approximated by the modified Buckingham potential (74) [17]. In particular for the calculated potential curves

$X^2\Sigma_{1/2}$, $A^2\Pi_{3/2}$ and $B^2\Sigma_{1/2}$ the parameters of this approximation are as follows: $X^2\Sigma_{1/2}$, $\mathbf{A}$ = 116.869 eV, α = 1.654 Å^{-1}, $\mathbf{C_6}$ = 946.502 eV× Å^6, $\boldsymbol{R_0}$ = 1.504 Å; $A^2P_{3/2}$, $\mathbf{A}$ = 3214.79 eV, $\boldsymbol{\alpha}$ = 3.185 Å^{-1}, $\mathbf{C_6}$ = 22.774 eV× Å^6, $\boldsymbol{R_0}$ = 1.960 Å; $B^2\Sigma_{1/2}$, $\mathbf{A}$ = 102.829 eV, $\boldsymbol{\alpha}$ = 1.256 Å^{-1}, $\mathbf{C_6}$ = 3408.543 eV× Å^6, $\boldsymbol{R_0}$ = 1.566 Å.

Thus modified Buckingam potentials could be used in formulating the explicit procedure for the line contour calculations.

5.4. Unified Franck-Condon Theory in the Binary Approximation

The Unified Franck-Condon Theory (UFCT) of the spectral line broadening (see [8, 14-15] and references therein) describes the whole line contour and provides the convenient tool for practical calculations. We remind that the basing point of any unified theory is the usage of a binary approximation, in which the line contour is represented in the Lorentz-like form with the line halfwidth in the nominator depending on the frequency of radiation and the impact value of the line halfwidth in the denominator [8, 14-15, 64]. In fact in the UFCT line contour is defined as the normalized spectral distribution of radiative transition in the compound system – radiator + perturber [8, 14-15, 64]. The kind of the unified theory used below is characterized by the implementation of Frank-Condon principle so familiar in consideration of transitions in molecular spectra [14-15]. So, UFCT is constructed in the case, when only the binary collisions are of importance. In the UFCT the non-adiabatic effects are neglected at large distances, and the adiabatic dispersion potentials are used (see discussion at the end of the subsection **5.2**). The relative contribution of the different initial and final electronic states of the quasi-molecules A-X to the spectra is described by the statistical weight $g(i\rightarrow f)$ assigned to each pair $U_i(R)$ and $U_f(R)$ of interaction potential curves and given by the expression

$$g(i \rightarrow f) = \frac{N(i \rightarrow f)_{AX}}{N(i_A \rightarrow f_A)} \tag{75}$$

Here $N(i \rightarrow f)_{AX}$ is the number of the allowed dipole transitions with $\Delta\Omega = 0, \pm 1$ (Ω is the projection of the quasi-molecular electronic angular momentum on internuclear axis) between quasi-molecular electronic states corresponding to the potential curves $U_i(R)$, and $U_f(R)$ and $N(i_A \rightarrow f_A)$ is the total number of the allowed dipole transitions $i_A \rightarrow f_A$ with $m_i - m_f = 0, \pm 1$ (m_i, m_f are magnetic quantum numbers of A) in a free radiating atom A. The latter rule could be illustrated by broadening of the most intensive Tl or In lines by Xe or Zn. The final lower states for given A (Tl or In) are $^2P_{j=1/2;3/2}$ (one p-electron) and initial upper state is $^2S_{1/2}$ (one s-electron). The upper $B^2\Sigma_{1/2}$ state of the quasi-molecule A-X correlates with the $^2S_{1/2}$ state of A. The lower quasi-molecular states $A^2\Sigma_{1/2}$ and $X^2\Pi_{3/2}$ correlate with the state $^2P_{3/2}$ of A, while the lower quasi-molecular state $X^2\Pi_{1/2}$ correlates with the atomic state $^2P_{1/2}$. For the atomic transition $^2S_{1/2} \rightarrow {}^2P_{3/2}$ we have that $N(^2S_{1/2} \rightarrow {}^2P_{3/2}) = 6$, $N(B^2\Sigma_{1/2} \rightarrow A^2\Sigma_{1/2}) = 4$, $N(B^2\Sigma_{1/2} \rightarrow X^2\Pi_{3/2}) = 2$ and therefore $g\,(B^2\Sigma_{1/2} \rightarrow A^2\Sigma_{1/2}) = 2/3$, $g\,(B^2\Sigma_{1/2} \rightarrow X^2\Pi_{3/2}) = 1/3$. For the atomic transition $^2S_{1/2} \rightarrow {}^2P_{3/2}$ we have that $N(^2S_{1/2} \rightarrow {}^2P_{1/2}) = 4$, $N(B^2\Sigma_{1/2} \rightarrow X^2\Pi_{1/2}) = 4$ and therefore $g\,(B^2S_{1/2} \rightarrow X^2\Pi_{1/2}) = 1$.

It will be assumed for all quasi-molecular potentials of interest ($\gamma = i, f$), that the temperature is sufficiently high, so, that the inequality takes place

$$k_B T >> D_{e,\gamma}, \tag{76}$$

where $D_{e,\gamma}$ is the depth of the well of the potential $U_\gamma(R)$ (see Fig. 7 – Fig. 9).

Additionally for rather heavy atomic particles the semiclassical approximation is applicable for the description of the relative translational motion. In this approximation the difference of relative motions of A and X in the fields of the potentials $U_i(R)$ and $U_f(R)$ could be neglected and described by a trajectory in the field of some "mean" potential $U_0(R)$.

Neglecting line shift, UFCT gives the following expression for the normalized contour $F(\Delta\omega)$

$$F(\Delta\omega) = \frac{1}{\pi} \frac{\Phi(\Delta\omega)}{(\Delta\omega)^2 + (\Delta\omega_{1/2}^{(imp)})^2} \tag{77}$$

Here $\Delta\omega$ is the detuning of cyclic frequency

$$\Delta\omega = \omega - \omega_{if}, \tag{78}$$

ω is the cyclic frequency of radiation, ω_{if} is the unperturbed cyclic frequency of transition $i \to f$ of the free atom A, $\Delta\omega_{1/2}^{(\mathrm{imp})}$ is the impact halfwidth of the Lorentz line profile (subsection 5.2, Eq. (73)). Due to the unified theory expressions for the line shape like (77) the integral radiation of the transition is determined almost completely by the Lorentz impact center of the contour. Within formulated above assumptions

$$\Phi(\Delta\omega) = \sum_{if} g(i \to f)\, \Phi_{if}(\Delta\omega),$$

$$\Phi_{if}(\Delta\omega) = \pi\, n_{\mathrm{X}} \langle u \rangle \int_0^\infty \frac{\varepsilon\, \mathrm{d}\varepsilon}{(k_{\mathrm{B}}T)^2} \exp\left(-\frac{\varepsilon}{k_{\mathrm{B}}T}\right) \times \int_0^\infty 2b\, \mathrm{d}b\, G_{if}(b, \varepsilon, \Delta\omega)^2, \tag{79}$$

where ε is the energy of relative A-X motion, b is the impact parameter of the A-X trajectory of relative motion. The reduced Franck-Condon factor $G_{if}(b, \varepsilon, \Delta\omega)$ has the form

$$G_{if}(b, \varepsilon, \Delta\omega) = \frac{2}{\hbar} \int_0^\infty \mathrm{d}t\ \Delta U_{if}\left[R(t, b, \varepsilon)\right] \cos\left[\Delta\omega\, t - \eta_{if}(t, b, \varepsilon)\right], \tag{80}$$

$$\Delta U_{if}(R) = U_i(R) - U_f(R), \tag{81}$$

where $\eta_{if}(t, b, \varepsilon)$ is the phase shift versus the relative A-X motion with the initial kinetic energy ε_i and the impact parameter b along the trajectory $R(t, b, e_i)$

$$\eta_{if}(t, b, \varepsilon) = \frac{1}{\hbar} \int_0^t \Delta U_{if}\left[R(t', b, \varepsilon)\right] \mathrm{d}t' \tag{82}$$

The trajectory is determined in some mean interaction potential $U_0(r)$**,** chosen on physical grounds. The integration over ε in (79) represents the average over equilibrium Maxwell distribution. As it could be concluded from (80) the dipole moment of quasi-molecular transition is assumed to vary very slowly versus r. So, it could be put as constant, factored out and canceled during the normalization of the profile.

5.5. Double-range Expression for Line Shape

For a given pair of quasi-molecular initial and final states the reduced Franck-Condon factors and corresponding line contour are determined by the interaction potentials $U_i(R)$ and $U_f(R)$ and the common trajectory $R(t, b, \varepsilon)$. The potentials $U_{i,f}(R)$ have a repulsive exponential part, a Van der Waals potential well and an attractive dispersion tail (see (74) and Fig. 6). Having in mind assumption (72), only the repulsive part of potentials $U_i(R)$ and $U_f(R)$ could be taken into account in constructing the "mean" potential $U_0(R)$ in the range of sufficiently small R. It is reasonable to accept for it the purely exponential form

$$U_0(R) = A_0 \exp(-\alpha_0 R);\ A_0 = \sqrt{A_i A_f}\ ,\ \alpha_0 = \frac{\alpha_i + \alpha_f}{2}. \tag{83}$$

Here $A_{i,f}$, $\alpha_{I,f}$ are parameters of the approximation of the potential $U_{i,f}(R)$ by the modified Buckingam potential (74). Since the potential $U_0(R)$ decrease very rapidly with R, trajectories in this potential can be divided into two groups: *the trajectories $R^{(1)}(t, b, \varepsilon)$ with impact parameters $0 \le b \le R_0$, ** and the trjaectories $R^{(2)}(t, b, e)$ with impact parameters $b > R_0$. The value of R_0 is chosen large enough to consider the trajectories $R^{(2)}(t, b, e)$ as rectilinear

$$R^{(2)}(t, b, \varepsilon) = \sqrt{b^2 + u^2 t^2} \tag{84}$$

where u is the relative velocity of A and X atoms at infinite separation. Since $U_0(r)$ decrease very rapidly with R, R_0 should be close to the turning distance at $b = 0$. A reasonable choice for temperature T is

$$R_0 = \frac{1}{\alpha_0}\left[\ln\left(\frac{A_0}{k_B T}\right) + 0.577216\right], \tag{85}$$

where the figure inside square brackets is the Euler's constant. For trajectories $R^{(1)}(t, b, \varepsilon_i)$ due to the short range character of potential $U_0(R)$ the Takayanagi modified wave number approximation [71] could be used, which gives

$$R^{(1)}(t,b,\varepsilon) = R_{t,0}\left[\varepsilon_{mwn}(\varepsilon,b)\right] + \frac{2}{\alpha_0}\ln\left\{\mathrm{ch}\left[\frac{\alpha_0\, u_{mwn}(\varepsilon,b)t}{2}\right]\right\}, \tag{86}$$

$$\varepsilon_{mwn}(\varepsilon,b) = \varepsilon - \frac{\varepsilon b^2}{R_0^2},$$

$$R_{t,0}\left[\varepsilon_{mwn}(\varepsilon,b)\right] = \frac{1}{\alpha_0}\ln\left[\frac{A_0}{\varepsilon_{mwn}(\varepsilon,b)}\right], u_{mwn}(\varepsilon,b) = \sqrt{2\varepsilon_{mwn}(\varepsilon,b)/\mu}$$

According to separation of trajectories in two types, $\Phi_{if}(\Delta\omega)$ in (77) is expressed as the sum of two terms, corresponding to the two ranges of impact parameters

$$\Phi_{if}(\Delta\omega) = \Phi_{if}^{(1)}(\Delta\omega) + \Phi_{if}^{(2)}(\Delta\omega)\,. \tag{87}$$

The trajectories $R^{(1)}(t, b, e_i)$ give the following contribution

$$\Phi_{if}^{(1)}(\Delta\omega) = \pi\, n_X \langle u\rangle R_0^2 \int_0^\infty \frac{\varepsilon\, d\varepsilon}{(k_B T)^2}\; G_{if}^{(1)}(\varepsilon,\Delta\omega)^2 \exp\left(-\frac{\varepsilon}{k_B T}\right) \tag{88}$$

Here

$$G_{if}^{(1)}(\varepsilon,\Delta\omega) = \frac{2}{\hbar}\int_0^\infty dt\, \Delta U_{if}\left[R^{(1)}(t,b=0,\varepsilon)\right]\cos\left[\Delta\omega t - \eta_{if}^{(1)}(t,\varepsilon)\right],$$

$$\eta_{if}^{(1)}(t,\varepsilon) = \frac{1}{\hbar}\int_0^\infty dt'\, \Delta U_{if}\left[R^{(1)}(t',b=0,\varepsilon)\right] \tag{89}$$

On the other hand, in the contribution from trajectories $R^{(2)}(t, b, \varepsilon_i)$ the integration over b can not be performed in the general form and the following formula can be considered as a final one

$$\Phi_{if}^{(2)}(\Delta\omega) = \pi\, n_X \langle u\rangle \int_0^\infty \frac{\varepsilon\, d\varepsilon}{(k_B T)^2}\exp\left(-\frac{\varepsilon}{k_B T}\right) \times \int_{R_0}^\infty db\; 2b\; G_{if}^{(2)}(b,\varepsilon,\Delta\omega)^2 \tag{90}$$

Here

$$G_{if}^{(2)}(b,\varepsilon,\Delta\omega) = \frac{2}{\hbar}\int_0^\infty dt\, \Delta U_{if}\left(\sqrt{b^2+u^2t^2}\right)\cos\left[\Delta\omega t - \eta_{if}^{(2)}(t,\varepsilon,b)\right],$$

$$\eta_{if}^{(2)}(t,\varepsilon,b) = \frac{1}{\hbar}\int_0^t dt'\, \Delta U_{if}\left(\sqrt{b^2+u^2t'^2}\right) \tag{91}$$

5.6. Massey Parameter and Wings of the Line Profile

Let us consider the qualitative behavior of $\Phi_{if}(\Delta\omega)$ for one pair of the initial $U_i(R)$ and final $U_f(R)$ potential curves. The idea of this consideration is based upon the fact that $G_{if}(b, \varepsilon, \Delta\omega)$ (80) has the form of Fourier transform at the detuning of cyclic frequency $\Delta\omega$ of the smooth function $\Delta U_{if}\left[R(t,b,\varepsilon)\right] \exp\left[i\eta_{if}(t,b,\varepsilon)\right]$ of time t. Therefore (see, e.g. [5]) behavior of $G_{if}(b, \varepsilon, \Delta, \omega)$ as a function of $\Delta\omega$ is governed by the so called Massey parameter $\xi(\Delta\omega, b, \varepsilon)$

$$\xi(\Delta\omega, b, \varepsilon) = |\Delta\omega|\,\tau(b, \varepsilon)\,, \tag{92}$$

where $\tau(b, \varepsilon)$ is the characteristic variation time of $\Delta U_{if}\left[R(t,b,\varepsilon)\right] \exp\left[i\eta_{if}(t,b,\varepsilon)\right]$. The Lorentz center of the profile corresponds to small enough $|\Delta\omega|$, where $\xi(\Delta\omega, b, \varepsilon) < 1$ for the wide range of impact parameters and $\varepsilon \sim k_B T$. The wings of the profile correspond to large $|\Delta\omega|$, where $\xi(\Delta\omega, b, \varepsilon) > 1$ for the wide range of impact parameters and $\varepsilon \sim k_B T$. If $\xi(\Delta\omega, b, \varepsilon) > 1$, the stationary phase approximation could be applied to evaluate the integral (80). In this approximation the value of integral (80) is determined by the values of the integrand in the vicinity of the stationary phase point $t_c(\Delta\omega, b, \varepsilon)$, which is the root of the equation

$$\Delta\omega = \frac{1}{\hbar}\Delta U_{if}\left[R(t,b,\varepsilon)\right] \tag{93}$$

Thus the behavior of the interaction potential difference $\Delta U_{if}(R)$ determines the behavior of the profile red wing. The consideration of many specific systems have shown that for strong transitions in the visible and ultraviolet ranges $\Delta U_{if}(R)$ behaves qualitatively analogously to this function, obtained in our quantum chemical calculations of the Na-Xe system, see Fig. 2 (a, b).

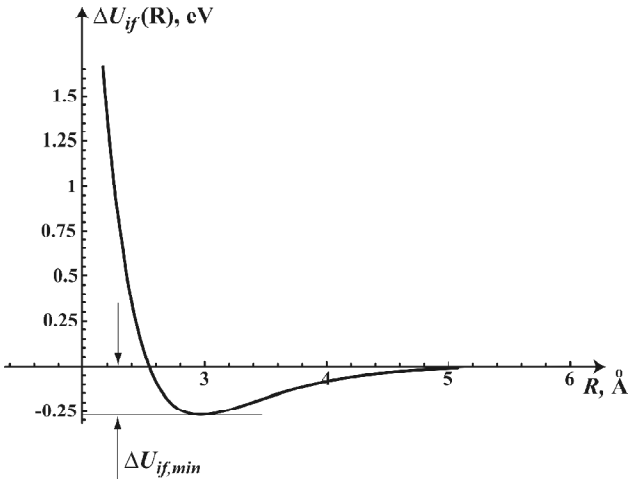

Figure 8: Interaction potential difference $\Delta U_{if}(R)$ for Na-Xe system ($i = A^2\Pi_{3/2}$, $f = X^2\Sigma_{1/2}$, advise corresponding data in the subsection 4.1)

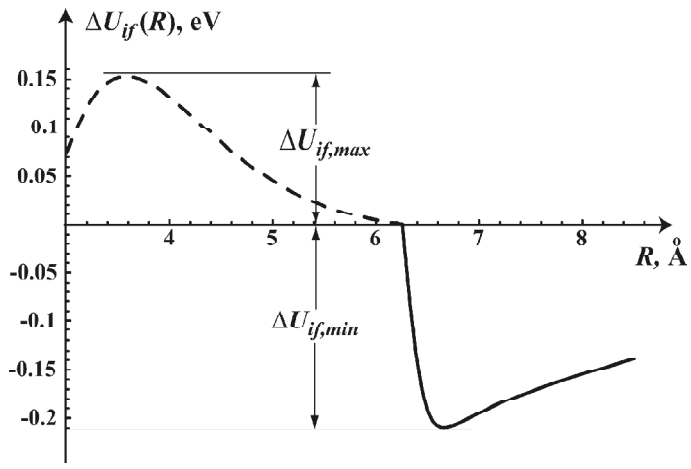

Figure 9: Interaction potential difference $\Delta U_{if}(R)$ for the Na-Xe system ($i = B^2\Sigma_{1/2}$, $f = X^2\Sigma_{1/2}$, advise corresponding data in the subsection 4.1). Dashed line - $\Delta U_{if}(R)$, solid line - $100 \times \Delta U_{if}(R)$

It is seen from Figs. 8 and 9, that for negative $\Delta\omega$ (red wing of the line) equation (93) has real roots only in the limited range of $\Delta\omega$ variation

$$\Delta\omega > \frac{1}{\hbar}\Delta U_{if,min}\,. \tag{94}$$

If $\Delta\omega < \frac{1}{\hbar}\Delta U_{if,min}$, then roots of equation (93) are complex, and corresponding $G_{if}(b, \varepsilon, \Delta\omega)$ decreases exponentially $\propto \exp[-\xi(\Delta\omega, b, \varepsilon)]$ with decreasing $\Delta\omega$. As for positive $\Delta\omega$ (blue wing of the line) situation is

different. It is seen from Figs. 8 and 9, that two situations may exist here depending on the specific interaction potentials. The range of positive $\Delta\omega$ for which equation (93) has real solution may be practically unrestricted (Fig. 8) or restricted from above (Fig. 8)

$$\Delta\omega < \frac{1}{\hbar}\Delta U_{if,max}. \tag{95}$$

If there maximum of $\Delta U_{if}(R)$ exists as in Fig. 9, then for $\Delta\omega > \frac{1}{\hbar}\Delta U_{if,max}$ the roots of equation (93) are complex, and corresponding $G_{if}(b, \varepsilon, \Delta\omega)$ decreases exponentially $\propto \exp[-\xi(\Delta\omega, b, \varepsilon)]$ with increasing $\Delta\omega$. It is to be noted that if maximum of $\Delta U_{if}(R)$ exists, and always

$$\Delta U_{if,max} > |\Delta U_{if,min}|. \tag{96}$$

Based on the described here connection between the Massey parameter and profile wings together with the double range expression for the line profile, introduced in the subsection 5.5, it is possible to formulate the physically reasonable grounds for cutting procedure, the goals of which were pointed out in 5.1. Recommendations concerning the form of the wings profile and cutting of these wings which are given below refer to strong dipole allowed lines in the visible and ultraviolet spectral ranges for which

$$b_W > R_0. \tag{97}$$

Here

$$b_{\mathrm{W}} = \left(\frac{3\pi\left|C_{6,i} - C_{6,f}\right|}{8\hbar\langle u\rangle}\right)^{1/5} \tag{98}$$

is the more definite definition of Weisskopf radius [7], which determines impact width $\Delta\omega_{1/2}^{(\mathrm{imp})}$ mentioned in **5.1**.

5.6.1. Red Wing

The minimum of $\Delta U_{if}(R)$ practically always occurs at

$$R > R_0. \tag{99}$$

Therefore trajectories, which give the main contribution to $\Phi_{if}(\Delta\omega)$ at negative $\Delta\omega$, satisfying (94), belong to the group 2, defined in the previous subsection 5.5. (function $\Phi_{if}^{(2)}(\Delta\omega)$ in (87)). For these trajectories the unique Massey parameter

$$\xi_2 = \left|\Delta\omega\right|\tau_2; \tau_2 = \frac{b_{\mathrm{W}}}{\langle u\rangle}, \tag{100}$$

could be introduced. Having in mind the definition of Massey parameter (100) and the above reasoning (see (92), (93)), it could be concluded that the red wing of line contour corresponds to negative $\Delta\omega$ such that

$$\frac{1}{\hbar}\left|\Delta U_{if,min}\right| > |\Delta\omega| > \frac{\langle u\rangle}{b_{\mathrm{W}}} \tag{101}$$

It is shown in [14, 15] that this part of the red wing is described by the expression of classical statistical distribution for $\Delta U_{if}(R) \propto R^{-6}$. At $\Delta\omega = \Delta U_{if,min}/\hbar$ the red satellites appears. As mentioned above for negative $\Delta\omega < \frac{1}{\hbar}\Delta U_{if,min}$ the equation (93) has no real roots and therefore the function $\Phi_{if}^{(2)}(\Delta\omega)$, which gives here the main

contribution, decreases exponentially with the decreasing $\Delta\omega$. As according to the approximate conventional procedure [62] the profile red wing consists of the Lorentz and classical statistical parts calculated for the dispersion potentials, it could be concluded that the red wing of this profile should be cut at some value $\Delta\omega_{c,red}$. It could be recommended to accept

$$\Delta\omega_{c,red} = \frac{1}{\hbar}\left|\Delta U_{min,eff}\right|, \tag{102}$$

where $\Delta U_{min,eff}$ is some average minimum value of the differences of the potentials of the pair of initial and final states. The value of $\Delta\omega_{c,red}$ is specific for each pair A-X and could be estimated from approximate potential curves, including attractive and repulsive parts. For the systems of interest $\Delta\omega_{c,red}$ may vary in the wide range from hundreds to thousands of cm^{-1}.

5.6.2. Blue Wing

The interaction potential difference $\Delta U_{if}(R)$ usually assumes positive values at

$$R < R_0. \tag{103}$$

Therefore the main contribution to the blue wing is given by the trajectories with Massey parameter $\xi(\Delta\omega, b, \varepsilon)$, which belong to the group 1, defined in the subsection 5.5 (function $\Phi_{if}^{(1)}(\Delta\omega)$ in (93)). For these trajectories the unique Massey parameter

$$\xi_1 = \Delta\omega\,\tau_1,\ \tau_1 = \frac{1}{\alpha_0\langle u\rangle}, \tag{104}$$

could be introduced. Correspondingly in the range of positive $\Delta\omega$ such that

$$\frac{1}{\hbar}\Delta U_{if,max} > \Delta\omega > \alpha_0\langle u\rangle \tag{105}$$

the stationary phase method can be applied to estimate $\Phi_{if}^{(1)}(\Delta\omega)$. With increasing $\Delta\omega$ equation (93) will have real roots for trajectories with increasing energy. This will lead to exponential decrease of $\Phi_{if}^{(1)}(\Delta\omega)$ with increasing $\Delta\omega$ due to thermal averaging in (88). If $\Delta U_{if}(r)$ have maximum, as it is shown in Fig. 8, the blue satellite at

$$\Delta\omega = \Delta U_{if,\max} \tag{106}$$

will appear. It is to be noted that this satellite is usually very far from the center of the line (up to several thousands of cm^{-1}). Thus the far blue wing shape may be rather complicated, but for $\Delta\omega > \alpha_0\langle u\rangle$ it decreases very rapidly (approximately exponentially). Therefore it could be recommended to accept the cutting of the blue wing at

$$\Delta\omega_{c,blue} = \alpha_0\langle u\rangle. \tag{107}$$

Typically α_0 is about 2-3 $Å^{-1}$.

In summary, it could be stated, that for the binary case in the adiabatic approximation the difference between semi-empirical and MB and QC results is reduced due to small value of the power index 2/5. This still holds even if to take into account the degeneracy influence on the impact broadening by atoms within MB and the consideration of repulsive part of potential at small distances [17, 24].

6. SUMMARY AND DISCUSSION

The calculation methods of Van der Waals interactions of atomic pairs and broadening coefficients are considered. It is demonstrated by comparison with the approach using $\langle r^2\rangle$, evaluated with the help of Green-Selin-Zachor

approximation, Molecular Basis approach and *ab initio* Electron Modeling calculations, that Hydrogen Like Approximation provides satisfactorily accurate results for description of broadening coefficients in the adiabatic approximation. It is shown that allowance for the degeneracy in Molecular Basis provides functional dependence of broadening coefficients versus angular momentum quantum numbers of the initial and final states. However, in the adiabatic approximation the discrepancy between HLA values of broadening coefficients and those obtained in the Molecular Basis with the allowance for the degeneracy turns out to be of the order of unity and thus insignificant. In particular it became possible due to the first rigorous derivation of Van der Waals broadening in the impact regime with the allowance for the degeneracy within Molecular Basis in quasi-classical approximation, presented in the subsection 5.2 above.

The tables of Van der Waals broadening coefficients and C_6 calculated in HLA for known significant spectral lines of Ca, Ce, In, Na, Nd, Tl, Zn neutral radiators and various perturbers in the ground state are presented in Appendix [72]. The analogous tables, illustrating the application of additional GSZ approximation, are also available for several radiator-perturber pairs [73].

The main reason of using the HLA approximation consists in its relative simplicity on the background of corresponding data bareness in literature and the significant computational expenditures of their formation using more sophisticated approaches. At the same time the HLA data by their construction provide rather a supremum for the Van der Waals interaction constants of atom-atom interaction. On the other hand as it could be deduced from the comparison with the data, obtained by *ab initio* Electron Modeling, the HLA overestimation of atoms interaction in the ground states is expressed strongly than for the case, when one of the atoms is in the excited state. Thus the latter circumstance could result in the underestimation of the Van der Waals interaction constants differences, entering the broadening coefficients. However, the more extensive generation of data within *ab initio* Electron Modeling and its additional comparison is needed to verify this property. Also it could be easily seen that the HLA data provide as well a supremum for the closure approximation due to the appearance in it the characteristic energetic ratios less than unity (see for instance subsection 4.4.2.) if to neglect originating from Molecular Basis the angular momentum dependence factors of the order of unity. At last comparing GSZ values of $<r^2>$ with HLA ones (for Na [73]) it could be seen that the latter are systematically a bit larger. This confirms once more the evident HLA property of the largest electron orbit and the above consideration of relations between values of data, obtained within presented here different approaches.

7. APPENDIXES

I. Extended MCP-QZP valence basis set on Tl atom used in the present calculations

Table
Extended MCP-QZP valence basis set on Tl atom used in the present calculations: a -are Gaussian exponents; C- are *contraction* (i.e. *linear combinations*) coefficients

S-shells		*P-shells*		*D-shells*		*F-shells*		*G-shells*	
α	*C*	α	*C*	α	*C*	α	*C*	α	*C*
4986.3	-0.0146	563.481	0.01042	313.586	0.02534	20.3622	-0.0712	0.42677	0.68611
154.584	0.07478	42.4226	-0.0448	84.0453	0.10561	0.39524	0.99767	0.17948	0.42206
34.4978	-0.2037	8.99757	0.11873	14.1028	-0.1041				
6.63095	0.44783	1.6261	-0.2014	8.79927	-0.226	0.14053	1	0.07	1
1.67802	-0.4482	0.85977	-0.0807	1.66547	0.49602				
0.86195	-0.4159			0.65293	0.49727	0.056	1	0.028	1
		0.46163	1	0.23268	0.1743				
0.6125	1					0.022	1		
		0.18465	1	0.44968	1				
0.24501	1					0.01	1		
		0.0711	1	1.50434	-0.0962				
0.11426	1			0.24269	1.0222				
		0.0279	1						

table contd.

0.04915	1			0.1	1
		0.0112	1		
0.0196	1			0.04	1
		0.0045	1		
0.00784	1			0.016	1
		0.0018	1		
0.003	1			0.0064	1
				0.0025	1
				0.001	1

II. Van der Waals broadening of LaI spectral lines

Atomic data for La

The strong identified lines of Lanthanum in the wavelengths range λ~ 3500 - 5500 Å were analyzed, and corresponding Einstein coefficients were estimated. The evaluation of the dispersion interaction between La and noble gas atoms was started with one-electron atomic orbitals of La - 4f, 5d, 6s and 6p. The general characteristics of Lanthanum (La) are as follows: atomic number (Z) = 57, atomic weight = 138.9055, ground state = $[Xe]5d6s^2\ ^2D_{3/2}$, [Xe] = [$1s^2\ 2s^2\ 2p^6\ 3s^2\ 3p^6\ 3d^{10}\ 4s^2\ 4p^6\ 4d^{10}\ 5s^2\ 5p^6$], ionization energy: 5.5769eV (44981cm^{-1}).

The data for 12 strong identified lines of Lanthanum lines based upon information from [39] is given in Table II-1. The notations are the same as in Table 6.

Table II-1
Identified Transitions in Lanthanum

Wavelength (Å)	*$A_{ki}(10^8 s^{-1})$*	*Configuration*	*Term*	*J*	*Level(cm^{-1})*
3574.43 [a)]	~0.4	$[Xe]5d6s^2$	$^2D^o$	3/2	0.000
		$[Xe]4f5d(^3D^o)6s$		3/2	27968.54
4060.33[a)]	~0.4	$[Xe]5d^2(^3F)6s$	^4F	9/2	4121.572
		$[Xe]4f5d(^3G_o)6s$	$^4G^o$	11/2	28743.24
4187.32[a)]	~0.6	$[Xe]5d6s^2$	$^2D^o$	3/2	0.000
		$[Xe]5d6s(^3D)6p$		5/2	23874.95
4280.27 [a)]	~0.6	$[Xe]5d6s^2$	$^2D^o$	5/2	1053.164
		$[Xe]4f5d(^1G^o)6s$		7/2	24409.68
4949.77	0.87	$[Xe]5d6s^2$	$^2D^o$	3/2	0.000
		$[Xe]5d6s(^1D)6p$		1/2	20197.34
5145.42 [a)]	~0.4	$[Xe]5d^2(^3F)6s$	^4F	5/2	3010.002
		$[Xe]5d^2(^3F)6p$	$^4D^o$	3/2	22439.36
5177.31 [a)]	~0.6	$[Xe]5d^2(^3F)6s$	^4F	7/2	3494.526
		$[Xe]5d^2(^3F)6p$	$^4D^o$	5/2	22804.25
5211.86 [a)]	~0.7	$[Xe]5d^2(^3F)6s$	^4F	9/2	4121.572
		$[Xe]5d^2(^3F)6p$	$^4D^o$	7/2	23303.26
5234.27 [a)]	~0.5	$[Xe]5d^2(^3F)6s$	$^4F^o$	9/2	4121.572
		$[Xe]5d6s(^3D)6p$		7/2	23221.10
5455.15 [a)]	~0.5	$[Xe]5d6s^2$	^2D	5/2	1053.164
		$[Xe]5d^2(^3F)6p$	$^2D^o$	5/2	19379.40
5501.34	0.529	$[Xe]5d6s^2$	^2D	3/2	0.000
		$[Xe]5d^2(^3F)6p$	$^2D^o$	3/2	18172.35
5791.34 [a)]	~0.5	$[Xe]5d^2(^3F)6s$	^4F	9/2	4121.572
		$[Xe]5d^2(^3F)6p$	$^4F^o$	9/2	21384.00

[a)] For these lines Einstein coefficients are roughly estimated based upon relative intensities from [4] and absolute values for the lines with λ = 4949.77 Å and 5501.34 Å

The set of strong identified radiation lines of La differs from the one considered in the subsection 4.4. for Nd. In the latter all strong identified radiation lines correspond to the transition of the electron from the excited 6p-state to the lower 6s-state, forming the closed $6s^2$ outer electronic shell of the ground electronic configuration. In La there are several types of strong transitions:

1. Transition of one electron from the excited 6p-state to the lower 6s-state forming the closed $6s^2$ outer electronic shell of the ground electronic configuration [Xe]$5d6s^2$ (lines with λ = 4187.32 Å, 4949.77 Å);
2. Transition of one electron from the excited 6p-state to the lower 5d-state forming the excited configuration [Xe]$5d^26s$ (line with λ = 5234.27 Å);
3. Transition of one electron from the excited [Xe]4f5d6s configuration to the lower excited configuration [Xe]$5d^26s$ (line with λ = 4060.33 Å);
4. Transition of one electron from the excited [Xe]$5d^26p$ configuration to the lower excited configuration [Xe]$5d^26s$ (lines with λ = 5145.42 Å, 5177.31 Å, 5211.86 Å, 5791.34 Å);
5. Formally one-electron transitions between the excited configuration [Xe]4f5d6s and ground configuration [Xe]$5d6s^2$, which in fact can not take place due to selection rule (line with λ = 3574.43 Å, 4280.27 Å);
6. Transitions [Xe]$5d^26p \rightarrow$ [Xe]$5d6s^2$, which can not be realized as one-electron transitions (lines with λ = 5455.15 Å, 5501.34 Å).

The existence of strong transitions of types 5 and 6 is a clear manifestation of the established fact, that in the excited states of lanthanide atoms the strong inter-configuration mixing takes place (see e.g. [74]). Therefore in those cases where such mixing is obviously important the calculations of dispersion interaction based upon simple approaches, assuming belonging of the radiating atom state to definite configuration, might give estimates only by the order of magnitude.

The Van-der-Waals interaction between La atom in the corresponding upper and lower configurations states of the radiative transition and noble gas atom X(^{1}S) is determined by the mean square radii for 4f-, 5d-, 6s-, and 6p-orbitals, and their effective excitation energies (see, e.g. [5]). These parameters were estimated using the following assumptions:1. the relativistic effects can be neglected since only the outer shells of La are of interest; 2. effective one-electron potential from [16] can be used to calculate 4f-, 5d-, 6s-, and 6p-orbitals of La; 3. the radial atomic orbitals in the potential from [16] can be determined variationally in the basis formed from Coulomb orbitals.

The calculated binding energies for 4f-, 5d-, 6s-, and 6p-orbitals and corresponding mean square radii are given in Table II-2. Table II-2 includes also the calculated in [49] with the use of relativistic linear response method from [50] the average La ground state polarizability. This polarizability was used to estimate effective excitation energy of 6s-shell based on the Slater-Kirkwood approximation [5, 24], requiring that calculated in the closure approximation mean polarizability of La coincides with result of calculation in [49].

Table II-2
Electronic Structure Parameters of La

	Orbital parameters			
Orbital	*4f*	*5d*	*6s*	*6p*
Binding energy, eV	23.0	7.9	5.7	3.4
Mean square radius,	0.3	1.9	5.7	10.1
	Ground configuration $5d6s^2$ average polarizability, Å^3			
	31.1			

Effective broadening parameters due to Van-der-Waals interaction between heavy noble gas atoms X and La

The general approach to the calculation of the Van-der-Waals interaction broadening parameters, the effective differences $\Delta C_{6,eff}$ were described in detail in the section 3 and the subsection 4.3. Here for the transitions, presented in Table II-1, the calculations of $\Delta C_{6,eff}$ were performed. The parameters $\Delta C_{6,eff}$ of broadening by Xe and Kr due to dispersion interaction of strong La lines corresponding to transitions [Xe]5d6s(^{3}D)6p, $j_i = 5/2 \rightarrow$ [Xe]5d6s^2, $j_f = 3/2$ and [Xe]5d6s(^{1}D)6p, $j_i = 1/2 \rightarrow$ [Xe]5d6s^2, $j_f = 3/2$ were evaluated. The calculated parameters $\Delta C_{6,eff}$ are presented also in the Table II 3. It is to be noted that the upper state of the transition [Xe]5d6s(^{3}D)6p, $j_i = 5/2 \rightarrow$ [Xe]5d6s^2, $j_f = 3/2$ is not completely defined. Several possible pairs of values of the total orbital angular momentum of the upper initial state L_i and total spin S_i could give $j_i = 5/2$. All corresponding broadening parameters are given in Table II 3. The data, presented in Table II 3, show that values of $\Delta C_{6,eff}$ are determined practically completely (deviation not higher than 2%) by electronic configurations of the upper and lower states of the radiating atoms. Therefore within the accuracy of the accepted approach, the broadening parameters for all the transitions [Xe]5d6s→[Xe]5d6s^2 could be considered as equal, namely $\Delta C_{6,eff} = 257$ a.u. (153 eV × Å^6) for Kr; $\Delta C_{6,eff} = 408$ a.u. (244 eV × Å^6) for Xe.

Table II 3
Strong La lines, its Einstein Coefficients A_{ki} and Broadening Parameters Due to Collisions with Kr and Xe

Transition	*Wavelength,Å*	A_{ki},$10^8 s^{-1}$	$\Delta C_{6,eff}$; *X=Kr, a.u. (eV × Å^6)*	$\Delta C_{6,eff}$; *X=Xe, a.u. (eV × Å^6)*
5d6s(^{3}D)6p, j_i=5/2 → 5d6s^2, j_f=3/2	4187.32	~0.6	256.9 (153.6); L_i=3, S_i=3/2	409.0 (244.6); L_i=3, S_i=3/2
			256.4 (153.4); L_i=3, S_i=1/2	408.3 (244.2); L_i=3, S_i=1/2
			257.9 (154.2); L_i=2, S_i=3/2	410.7 (245.6); L_i=2, S_i=3/2
			255.7 (152.9); L_i=2, S_i=1/2	407.3 (243.5); L_i=2, S_i=1/2
			257.7 (154.1); L_i=1, S_i=3/2	410.4 (245.4); L_i=1, S_i=3/2
5d6s(^{1}D)6p, j_i=1/2→ 5d6s^2, j_f=3/2	4949.77	0.87	257.9 (154.2)	410.7(245.6)

III. Tables of Van der Waals Broadening Coefficients

III-1. HLA Tables

The corresponding tables of Van der Waals broadening coefficients, calculated within **HLA** (see section **2**), are available on the link already cited above [72]. The tables represent the collection of files, each of which is associated with the certain radiator: Ca, Ce, In, Na, Nd, Tl, Zn. The perturbers are: Xe, Hg, Zn, Ar, I. The tables for the radiators Ce, Na and Zn in the first column give the values of energy for the lower levels of spectral lines, and in the second column for the upper ones. The third column of tables in each file contains values of wavelengths for considered transitions of the atomic radiators. The forth column presents the statistical weight of the lower level and the fifth column presents the one for upper level. The Einstein coefficients for corresponding transitions are given in the sixth column. In the next columns each marked by the specific perturber (Xe, Hg, Zn, Ar, or I) the difference of the Van Der Waals interaction coefficients of the upper and lower levels, calculated along with HLA in atomic units for every transitions, are collected. The next set of columns marked by the specific perturbers contains the impact broadening coefficients for temperature 5000 K, calculated within HLA in rad/second cm^3. And the last set of columns again marked by the specific perturbers contains the quasistatic broadening coefficients,

calculated within HLA in rad/second cm^6. The table for Ca is similar to the previous ones but contains additional columns (6th and 7th) with atomic configurations of the upper and lower levels. For comparison the table for Tl has the special column with the differences of the Van Der Waals interaction coefficients of the upper and lower levels, calculated for 4 transitions using ab initio methods of quantum chemistry (see section 4.2).

The impact broadening coefficients were calculated within HLA (section 2) with the help of adiabatic theory of broadening [7]

$$C_{imp} = 4.08 \left|\Delta C_6^{imp}\right|^{2/5} \left(8k_B T/\pi\mu\right)^{3/10} \tag{III-1}$$

Here T is the current temperature, μ is the reduced mass of radiating atom and atom of buffer gas (perturber particles), ΔC_6^{imp} is the difference of Van der Waals interaction HLA constants in the impact region. The corresponding half-width the Lorentz profile is

$$\Delta\omega_{1/2}^{imp} = C_{imp} N_b\,, \tag{III-2}$$

where N_b is the buffer gas concentration.

The quasistatic broadening constant due to the Van der Waals interaction with buffer gas is

$$C_{quas} = \left(\frac{4\pi}{3}\right)^2 \Delta C_6^{quas}\,, \tag{III-3}$$

where ΔC_6^{quas} is the difference of Van der Waals interaction HLA constants of the upper and lower levels in the quasistatic region. The characteristic magnitude of quasistatic broadening is

$$\Delta\omega_0 = C_{quas} N_b^2 \tag{III-4}$$

For the composition of buffer gases the corresponding magnitude of impact and quasistatic broadening could be evaluated as

$$\begin{aligned} \Delta\omega_{1/2}^{imp} &= \sum_i C_{imp}^{(i)} N_b^{(i)}\,, \\ \Delta\omega_0 &= \left(\sum_i \sqrt{C_{quas}^{(i)}}\, N_b^{(i)}\right)^2. \end{aligned} \tag{III-5}$$

As it follows from results of section 2, 3, 5 the difference between ΔC_6^{quas} and ΔC_6^{imp} in principle could be associated with dependences on the angular momentum quantum numbers.

From comparison of broadening coefficients, presented in HLA tables and calculated within MB method with account of angular momentum quantum numbers and within HLA, it is seen that between both approaches there is no discrepancy significant for practical applications. As about the ΔC_6 data for 4 Tl transitions, calculated by *ab initio* methods, they differ from corresponding HLA results by about 4%, 8%, 28,6% and 60% correspondingly from top to the bottom as they appear in the table. But again at the same time the difference in ΔC_6 even of 60% due to small power index will be strongly reduced for broadening coefficients and could not be considered as very significant to reject the implementation of HLA results.

It should be noted that in calculations of $\langle r^2 \rangle$ for *Ce*, In and Tl the contribution of three electrons from outer open (unfilled) shells were included, for Ca and Zn – 2 electrons, where as for Na the only one valence electron is taken into account. The table for Ca contains 1749 transitions, for Ce –910, for Na – 385, for Zn – 135, for In – 24 and for Tl – 18.

III-2. GSZ Tables

The link to GSZ tables of Van der Waals broadening coefficients was also already given above in [73]. The GSZ tables are organized in similar way as previous ones as based on the same general formula for C_6, where only MSR $<r^2>$ is calculated within GSZ approximation (see subsection 2.1), and the same formulas for broadening coefficients, presented above in III-1. These tables contain data for identified spectral lines of neutral Ce, Na and La. The perturbers are Xe and Kr. Evidently data for only few lines are given in the case of La due to just small number of completely identified transitions [39]. The calculations here were performed only for one valence electron (or several equivalent electrons). Thus the gain of accuracy with the help of GSZ approximation (see [16] and section 2.1) could be estimated only for Na data, for which given HLA results also include contribution of only one open valence shell. However, such comparison does not show strong deviations of both sets of data. In general GSZ tables are much less extensive than HLA ones, and were aimed to test the influence on MSR values the deviation of intra-atomic potential from the pure Coulomb one.

References

[1] C. Yubero, M. S. Dimitrijević, M. C. García, M. D. Calzada, *Spectrochimica Acta Part B* **62**, 169-176, (2007).

[2] M. Weiss, H. Schubert, S. Meier, M. Born, D. Reiter, M. Stroesser, *J. Phys. D* **38**, 3170-3174, (2005).

[3] M. Born, *J. Phys. D* **32**, 2492-2504, (1999).

[4] M. J. Jongerius, *J. Appl.Phys.* **62**, 3138-3149, (1987); *J. Phys. B* **20**, 3345- 3365, (1987).

[5] E. E. Nikitin, S. Ya. Umanskii, *Theory of Slow Atomic Collisions*, Springer, Heidelberg, 1984, 1-432.

[6] B. M. Smirnov, *Asymptotic Methods in Theory of Atomic Collisions*, Atomizdat, Moscow, 1973, 1-294. (*in Russian*).

[7] I.I. Sobelman, *Introduction to the Theory of Atomic Spectra*, Pergamon Press, Oxford - New York, 1972, 1–609.

[8] N. F. Allard, J. F. Keilkopf, *Rev. Mod. Phys.* **54**, 1103 - 1182 (1982); N.F. Allard, F. Allard, J. F. Keilkopf, *Astronomy & Astrophysics* **440**, 1195-1201, (2005).

[9] G. Peach, *J. Phys. B* **17**, 2599-2618 (1984); B.N.I. Al-Saqabi, G. Peach, *J. Phys. B* **20**, 1175-1191, (1987).

[10] F. Schuller, W. Behmenburg, *Phys. Reports* **4**, 273-334, (1974).

[11] *http://www.pmp.uni-hannover.de/cgi-bin/ssi/test/kurucz/sekur.html*

[12] *http://www.nist.gov/physlab/data/asd.cfm*

[13] E. Fitz, R.A. Marcus, *J. Chem.. Phys.* **59**, 4380–4392, (1973).

[14] J. Szudy, W. E. Baylis, *JQSRT* **15**, 641, (1975).

[15] J. Szudy, W. E. Baylis, *JQSRT* **17**, 681, (1977).

[16] A. E. S. Green, D. L. Sellin, A. S. Zachor, *Phys. Rev.* **184**, 1-9, (1969).

[17] R. A. Buckingham, *Proc. Roy. Soc.*, London. Series A, **168**, 264-283, (1938).

[18] Albrecht Unzöld, *Physik der Sternatmosphären*, 1938, Chapter XIII, 71, Eqs. (71.23) – (71.30) (in Russian translation - Foreign Literature Publishing House, Moscow, 1949, 306-307).

[19] R. S. Dygdala, *J. Phys. B* **21**, 2039-2047, (1988).

[20] A.A. Radzyg, B.M. Smirnov, *Reference Data on Atoms, Molecules and Ions*, Springer, Berlin- Heidelberg, 1985.

[21] C. Froese-Fischer, *Comput. Phys. Comm.* **4,** 107, (1972),

[22] J. P. Desclaux, *Comp. Phys. Comm.* **9,** 31, (1975).

[23] M. Marinescu, H. R. Sadeghpour, A. Dalgarno, *Phys. Rev. A* **49**, 982-988, (1994).

[24] J. O. Hirschfelder, C. F. Curtis, R. B. Bird, *Molecular Theory of Gases and Liquids*, Wiley, N.Y., 1954.

[25] D. C. S. Allison, P. G. Burke, W. D. Robb, *J. Phys. B* **5**, 1431, (1972).

[26] M. B. Doran, *J. Phys. B* **7**, 668, (1974),

[27] H. P. Kelly, *Int. J. Quant. Chem.* **3**, 349, (1970).

[28] M. A. Spackman, *J. Chem. Phys.* **94**, 1288 (1991); *ibid.* **94**, 1295, (1991),

[29] G. P. Arrighini, C. Guidotti, *Mol. Phys.* **28**, 273, (1974).

[30] V. Magnasco, M. Battezzati, R. Austi, *Chem. Phys. Lett.* **51**, 378, (1977).

[31] G. Onida, L. Reinig, A. Rubio, *Rev. Mod. Phys.* **74**, 601, (2002).

[32] M. A. L. Marques, E. K. U. Gross, *Annual Review of Physical Chemistry* **55,** 427-455, (2004).

[33] M. A. L. Marques, A. Castro, G. Malloci, G. Mulas, S. Botti, *J. Chem. Phys.* **127**, 014107, (2007).

[34] A. Dalgarno, W. S. Davison, *in Adv. Atom. Mol. Physics* **2**, ed. D.R. Bates, Academic Press, N.Y., 1966, 1-32.

[35] T. Y. Chang, *Rev. Mod. Phys.* **39**, 911, (1967).

[36] N. Geum, G. H. Jeung, A. Derevianko, R. Cote, A. Dalgarno, *J. Chem. Phys.* **115**, 5984, (2001).

[37] C. Zhu, A. Dalgarno, S.G. Porsev, A. Derevianko, *Phys. Rev. A* **70**, 032722, (2004).

[38] S. G. Porsev, A. Derevianko, *JETP* **102**, 195–205, (2006).

[39] J. E. Sansonetti, and W. C. Martin, *J. Phys. Chem. Ref. Data* **34**, 1559, (2005).

[40] B.O. Roos, Multiconfigurational Quantum Chemistry for Ground and Excited States, in *Radiation Induced Molecular Phenomena in Nucleic Acids*, M. K. Shukla, J. Leszczynski (eds.), Springer Science+Business Media B.V. (2008), 125-156.

[41] D. G. Fedorov, J.P. Finley, *Phys.Rev. A* **64**, 042502, (2001).

[42] W. C. Ermler, R. B. Ross, and P.A. Christiansen, *Advances in Quantum Chemistry* **19**, 139 - 182 (1988); *http://people.clarkson.edu/~pac/reps.html*

[43] *http://www.msg.ameslab.gov/GAMESS/GAMESS.html*

[44] E. Miyoshi, Y. Sakai, K. Tanaka, M. Masamura, *J. Mol. Struct. (THEOCHEM)* **451**, 73, (1998).

[45] T. Noro, M. Sekiya, Y. Osanai, E. Miyoshi, T. Koga, *J. Chem. Phys.* **119**, 5142, (2003).

[46] *http://setani.sci.hokudai.ac.jp/sapporo/Order.do*

[47] *http://physics.nist.gov/PhysRefData/Handbook/Tables/indiumtable5.htm*

[48] E. Miyoshi, H. Mori, R. Hirayama, Y. Osanai, T. Noro, H. Honda, M. Klobukowski, *J. Chem. Phys.* **122**, 074104, (2005).

[49] G. D. Doolen, Los Alamos National Laboratory report, unpublished.

[50] A. Zangwill, P. Soven, *Phys. Rev. A* **21**, 1561, (1980).

[51] A. R. Allouche, M. Aubert-Frecon, S.Ya. Umanskiy, *J. Chem. Phys.* **124**, 184317 (2006).

[52] M. Dolg, H. Stoll, A. Savin, H. Preuss, *Theor. Chim. Acta* **75**, 173, (1989).

[53] M. Dolg, H. Stoll, H. Preuss, *Theor. Chim. Acta* **85**, 441, (1993).

[54] A. Nicklass, M. Dolg, H. Stoll, H. Preuss, *J. Chem. Phys.* **102**, 8942, (1995).

[55] K. Raghavachari, G.W. Trucks, J.A. Pople, M. Head-Gordon, *Chem. Phys. Lett.* **157**, 479, (1989).

[56] H. Lischka, R. Shepard, I. Shavitt, R.M. Pitzer, M. Dallos, T. Müller, P.G. Szalay, F.B. Brown, R. Ahlrichs, H. Böhm, A. Chang, D. Comeau, R. Gdanitz, H. Dachsel, C. Ehrhardt, M. Ernzerhof, P. Höchtl, G.K.S. Irle, T. Kovar, V. Parasuk, M. Pepper, P. Scharf, H. Schiffer, M. Schindler, M. Schüler, M. Seth, E. Stahlberg, J.-G. Zhao, S. Yabushita, Z. Zhang, COLUMBUS, *Ab Initio* Electronic Structure Program, version 5.8 (2001).

[57] *http://www.univie.ac.at/columbus/*

[58] P. E. M. Siegbahn, *Chem. Phys. Lett.* **55**, 386, (1978).

[59] A. Zaitsevskii, E. A. Pazyuk, A. V. Stolyarov, O. Docenko, I. Klincare, O. Nikolayeva, M. Auzinsh, M. Tamanis, R. Ferber, *Phys. Rev. A* **71**, 012510, (2005).

[60] S. F. Boys, F. Bernardi, *Mol. Phys.* **19**, 553, (1970).

[61] H. Margenau, *Physical Review* **48**, 755, (1935).

[62] H. P. Stormberg, *J. Appl. Phys.* **51**, 1963, (1980).

[63] R. G. Breene, *Rev. Mod. Phys.* **29**, 94, (1957).

[64] S. Y. Chen, M. Takeo, *Rev. Mod. Phys.* **29**, 20, (1957).

[65] G. Peach, *Advances in Physics* **30**, 367, (1981).

[66] P. J. Brussard, H. A. Tolhoek, *Physica* **23**, 955, (1957).

[67] A. R. Edmonds, *Angular Momentum in Quantum Mechanics,* Princeton Press, New Jersey, 1957.

[68] L. Huwell, J. Maier, H. Pauly, *Journ. Chem. Phys.* **74**, 5613, (1981).

[69] L. Huwell, J. Maier, H. Pauly, *Journ. Chem. Phys.* **76**, 4691, (1982).

[70] R. E. M. Hedges, D. L. Drummond, A. Gallaher, *Phys. Rev. A* **6**, 1519, (1972).

[71] K. Takayanagi, *Progress in Theoretical Physics, Japan*, **8**, 497 (1952); *J. Phys. Soc. Japan* **14**, 75, (1959).

[72] *http://www.kintechlab.com/rd-service/e-data-center/data-classification/classification-gases/atomicmolecular-properties/spectroscopic-properties/van-der-waals-broadening-coefficients-for-atoms/hla/*

[73] *http://www.kintechlab.com/rd-service/e-data-center/data-classification/classification-gases/atomicmolecular-properties/spectroscopic-properties/van-der-waals-broadening-coefficients-for-atoms/gsz/*

[74] V. V. Flambaum, A. A. Gribakina, G. F. Gribakin, M. G. Kozlov, *Phys. Rev.* A **50**, 267, (1994).